1994-06

Lifetime and reentry prediction for the Petite Amateur Navy Satellite (PANSAT)

Cuff, Daniel J.

Monterey, California. Naval Postgraduate School

NAVAL POSTGRADUATE SCHOOL
Monterey, California

THESIS

LIFETIME AND REENTRY PREDICTION
FOR THE PETITE AMATEUR
NAVY SATELLITE (PANSAT)

by

Daniel J. Cuff

June, 1994

Thesis Advisor: I. Michael Ross

REPORT DOCUMENTATION PAGE

Form Approved OMB No. 0704

1. AGENCY USE ONLY *(Leave blank)*	2. REPORT DATE	3. REPORT TYPE AND DATES COVERED
	16 June 1994	Master's Thesis

4. TITLE AND SUBTITLE Lifetime and Reentry Prediction for the Petite Amateur Navy Satellite (PANSAT)	5. FUNDING NUMBERS
6. AUTHOR(S) Cuff, Daniel J.	
7. PERFORMING ORGANIZATION NAME(S) AND ADDRESS(ES) Naval Postgraduate School Monterey CA 93943-5000	8. PERFORMING ORGANIZATION REPORT NUMBER
9. SPONSORING/MONITORING AGENCY NAME(S) AND ADDRESS(ES)	10. SPONSORING/MONITORING AGENCY REPORT NUMBER

11. SUPPLEMENTARY NOTES The views expressed in this thesis are those of the author and do not reflect the official policy or position of the Department of Defense or the U.S. Government.

12a. DISTRIBUTION/AVAILABILITY STATEMENT	12b. DISTRIBUTION CODE
Approved for public release; distribution is unlimited.	A

13. ABSTRACT *(maximum 200 words)*

The Naval Postgraduate School (NPS) is developing a small satellite for digital communications in the amateur frequency band. The Petite Amateur Navy Satellite (PANSAT) will primarily act as an orbiting spread-spectrum communications laboratory, possesses neither an attitude control nor a propulsion system and is designed to "tumble" along its orbital path once it is released from the launch vehicle which is scheduled to be the Space Shuttle. An explaination of the many variables and assumptions affecting PANSAT is provided as insight for the lifetime and reentry predictions. Using a conservative approach, results from combining altitudes and inclinations from expected Space Shuttle missions, solar flux and magnetic indicies from three different sources, and the use of an orbital propagator program, LIFETIME 4.1, which was developed by Aerospace Corporation, attest that the minimum 2 year lifetime requirement for PANSAT will be met by 9 Shuttle missions between July 1996 and December 1997. A reentry analysis concluded that PANSAT will experience sufficient aerodynamic forces to cause structural failure and breakup during atmospheric reentry.

14. SUBJECT TERMS: PANSAT; Lifetime; Reentry Prediction; F10.7; Ap; Atmospheric Density; Ballistic Coefficient; Atmospheric Drag; Zonal Harmonics; Breakup; Survival	15. NUMBER OF PAGES 81
	16. PRICE CODE

17. SECURITY CLASSIFICATION OF REPORT	18. SECURITY CLASSIFICATION OF THIS PAGE	19. SECURITY CLASSIFICATION OF ABSTRACT	20. LIMITATION OF ABSTRACT
Unclassified	Unclassified	Unclassified	UL

NSN 7540-01-280-5500

Standard Form 298 (Rev. 2-89)

Prescribed by ANSI Std. 239-18

Approved for public release; distribution is unlimited.

LIFETIME AND REENTRY PREDICTION
FOR THE PETITE AMATEUR
NAVY SATELLITE (PANSAT)

by

Daniel J. Cuff
Lieutenant, United States Navy
B.S., Drexel University, 1985

Submitted in partial fulfillment
of the requirements for the degree of

MASTER OF SCIENCE IN ASTRONAUTICAL ENGINEERING

from the

NAVAL POSTGRADUATE SCHOOL
June 1994

Author: [redacted]
Daniel J. Cuff

Approved by: [redacted]
I. Michael Ross, Thesis Advisor

[redacted]
Sandra L. Scrivener, Second Reader

[redacted]
Daniel J. Collins, Chairman
Department of Aeronautics and Astronautics

ABSTRACT

The Naval Postgraduate School (NPS) is developing a small satellite for digital communications in the amateur frequency band. The Petite Amateur Navy Satellite (PANSAT) will primarily act as an orbiting spread-spectrum communications laboratory, possesses neither an attitude control nor a propulsion system and is designed to "tumble" along its orbital path once it is released from the launch vehicle which is scheduled to be the Space Shuttle. An explaination of the many variables and assumptions affecting PANSAT is provided as insight for the lifetime and reentry predictions. Using a conservative approach, results from combining altitudes and inclinations from expected Space Shuttle missions, solar flux and magnetic indicies from three different sources, and the use of an orbital propagator program, LIFETIME 4.1, which was developed by Aerospace Corporation, attest that the minimum 2 year lifetime requirement for PANSAT will be met by 9 Shuttle missions between July 1996 and December 1997. A reentry analysis concluded that PANSAT will experience sufficient aerodynamic forces to cause structural failure and breakup during atmospheric reentry.

TABLE OF CONTENTS

I. INTRODUCTION 1
A. PANSAT MISSION SUMMARY 1
B. PANSAT ORBIT INSERTION 3
1. Orbit Insertion Method 3
2. Space Shuttle Operations 4
C. PURPOSE OF STUDY 7
II. OVERVIEW 8
A. INTRODUCTION 8
B. ORBITAL FUNDAMENTALS 8
1. Satellite Equations of Motion 8
C. SATELLITE ENVIRONMENT 11
1. Introduction 11
2. The Earth's Atmosphere 12
3. Solar Physics 14
4. F10.7 15
5. Magnetic Index - Ap 16
6. Atmospheric Density 18
7. Coefficient of Drag 20
8. Ballistic Coefficient 21
9. Atmospheric Drag 22
10. Zonal Harmonics 25
11. Summary 27
III. LIFETIME 4.1 28
A. INTRODUCTION 28
B. PROGRAM DESCRIPTION 28
1. Simplified Semianalytic Theory 29

2. Reentry Prediction 31
3. Program Accuracy 32
4. LIFETIME Output 34
IV. RESULTS AND ANALYSIS 37
A. INTRODUCTION 37
B. ASSUMPTIONS 37
1. Space Shuttle 37
2. PANSAT Ballistic Coefficient 38
3. F10.7 and Ap Data 39
4. Release Point in Orbit 42
5. Atmospheric Density Model 43
6. Propagation and Reentry Data 43
C. LIFETIME INPUTS 44
D. LIFETIME RESULTS 45
1. Solar Flux and Magnetic Activity 45
2. Combining Data 46
V. PANSAT REENTRY 53
A. INTRODUCTION 53
B. PANSAT'S ORBITAL DECAY 54
1. Reentry 54
2. Aerodynamic Heating 56
3. Aerodynamic Loading 58
4. Structural Failure and Breakup 60
5. Survivability to Impact 63
VI. CONCLUSIONS AND RECOMMENDATIONS 65
LIST OF REFERENCES 68
INITIAL DISTRIBUTION LIST 70

LIST OF TABLES

TABLE 1 PROJECTED SPACE SHUTTLE MISSIONS 6

TABLE 2 PANSAT ORBITAL CHARACTERISITCS 12

TABLE 3 YEARS OF SOLAR CYCLES 21-25 15

TABLE 4 PANSAT ENVIRONMENT AND DECAY BASED ON MSIS86 25

TABLE 5 PROJECTED PANSAT LIFETIME 48

TABLE 6 ACCEPTABLE SPACE SHUTTLE MISSIONS 49

TABLE 7 PANSAT ORBITAL PARAMETERS WITH SPACE SHUTTLE INSERTION 50

TABLE 8 REQUIRED STARTING ALTITUDES FOR VARIOUS F10.7/AP 51

TABLE 9 STAGNATION TEMPERATURES 57

TABLE 10 MATERIAL MELTING TEMPERATURES 64

LIST OF FIGURES

Figure 1 PANSAT Mission Objectives 2
Figure 2 PANSAT Launch Sequence as a CAP Payload 3
Figure 3 Space Shuttle Payload Performance to Circular Orbit 4
Figure 4 Orbital Elements 10
Figure 5 Structural Breakdown of the Earth's Atmosphere 13
Figure 6 Observed Monthly Mean Radio Flux at 10.7 cm 17
Figure 7 Density vs. Altitude for Various F10.7 Values 20
Figure 8 Drag Effects on High Eccentricity Orbits 24
Figure 9 Earth's Zonal Harmonics 27
Figure 10 Illustration of Integration and Breakup Model 33
Figure 11 Illustration of Impact Footprint 33
Figure 12 Plot of PANSAT Perigee/Apogee Decay History 35
Figure 13 Groundtracks / Debris Impact Area 35
Figure 14 Vehicle Altitude Decay History 36
Figure 15 PANSAT Schedule 38
Figure 16 Observed and Predicted F10.7 and Ap Values 39
Figure 17 LIFETIME Unbiased Solar Cycle vs. Predicted Values (F10.7) 40
Figure 18 LIFETIME Unbiased Solar Cycle vs. Predicted Values (Ap) 40
Figure 19 NASA F10.7 Values vs. Predicted Values 41
Figure 20 NASA Ap Values vs. Predicted Values 41
Figure 21 Comparison of Extreme Values of F10.7 and Ap and Inclination 46
Figure 22 Satellite Lifetime as a Function of Altitude and Solar Flux 51
Figure 23 Orbit Lifetime vs. Starting Altitudes and F10.7 / Ap Values 52
Figure 24 Types of Reentry 55
Figure 25 Shockwave and Stagnation Temperature on a Reentering Vehicle 57
Figure 26 Heating Rate vs. Altitude for Varied Ballistic Coefficients 59

Figure 27 Deceleration and Heating Dependence on Density and Velocity 61
Figure 28 Load Factor vs. Altitude for Varied Ballistic Coefficients 62
Figure 29 Probability of Land Impact vs. Inclination Angle 66

ACKNOWLEDGMENTS

I would first like to express my gratitude to my thesis advisor, Prof. I. Michael Ross for the direction and guidance given me during this research. Next, I would like to thank Dr. C.C. Chao of Aerospace Corporation for providing technical support. Finally, I especially would like to thank my family and friends for their personal support and inspiration during my stay at the Naval Postgraduate School and throughout my Naval career.

I. INTRODUCTION

A. PANSAT MISSION SUMMARY

The Naval Postgraduate School (NPS) is developing a small satellite for digital, store and forward communications in the amateur frequency band. The Petite Amateur Navy Satellite (PANSAT) will primarily act as an orbiting, spread-spectrum communications laboratory for the students, faculty and staff at NPS and will also allow civilian usage for amateur ham radio enthusiasts.

The spacecraft will incorporate neither an attitude control system nor a propulsion system, and is designed assuming a "tumble" along its orbital path. The expected weight of the spacecraft will be 150 pounds with a maximum diameter of 18.62 inches. The primary material will be aluminum 6061-T6 for the structure, silicon based solar cells for power production, control boards for the internal circuits, and nickel-cadmium batteries for stored energy. To provide 2-way communication, 4 omni-directional antennas will be attached to the outside structure. The proposed operational frequency is centered at 436.5 MHz with a spread of 2.5 MHz. Data can be transmitted at a bit rate of 9600 bits per second and up to 4MB of message storage is possible on board to the spacecraft's computer.

The spacecraft will be launched by the Space Shuttle by means of the Hitchhiker program. Using the design constraints for a Shuttle Small Self-Contained Payload

(SSCP), PANSAT vehicle will fly in the Get-Away Special (GAS) canister in the shuttle payload bay.

The objectives of the PANSAT program are as follows:

1. To provide NPS students, faculty and staff with educational hands-on experience in the design, development, integration, and operation of a low cost satellite.
2. PANSAT is classified as an amateur platform which allows legitimate access to the amateur UHF frequency band. The amateur radio community will have an opportunity to operate with spread spectrum communications in a real time or forward mode.
3. PANSAT will act as an on-orbit laboratory for telemetry and command operations.

Figure 1 provides a pictorial summary of PANSAT's objectives.

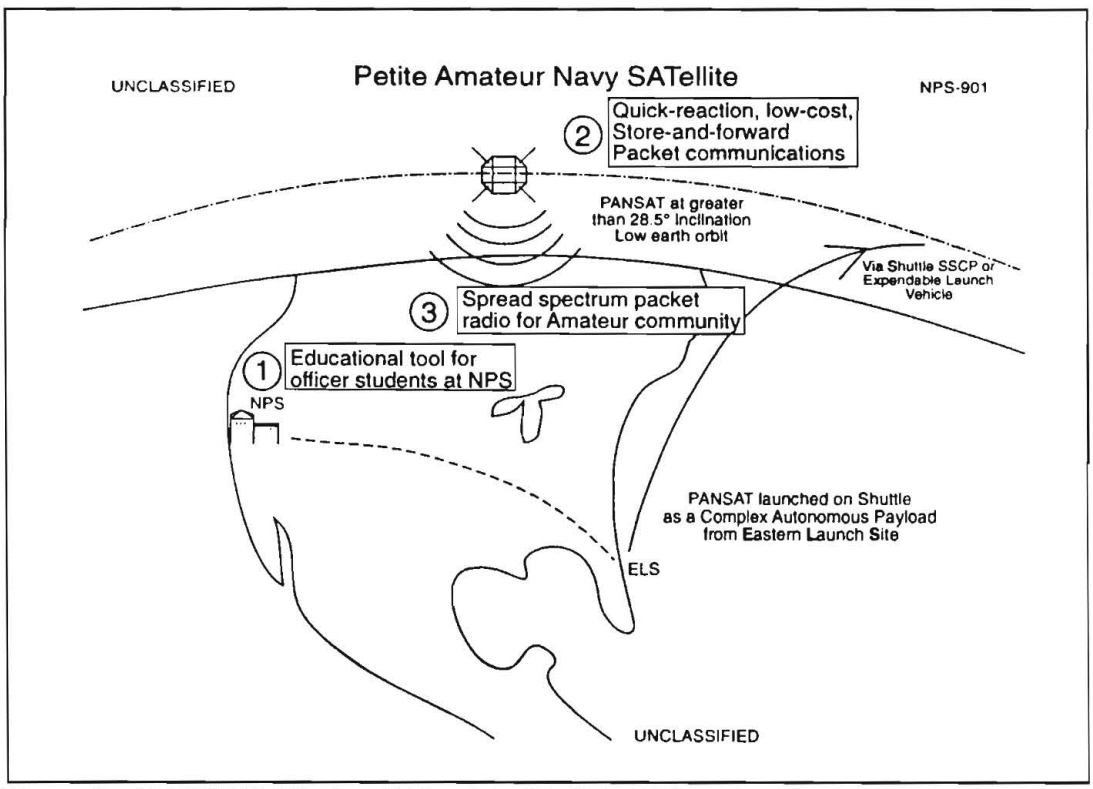

Figure 1. PANSAT Mission Objectives [Ref. 1:p. 2]

B. PANSAT ORBIT INSERTION

1. Orbit Insertion Method

As previously mentioned, PANSAT is adapted to the Space Shuttle Small Self-Contained Payload (SSCP) program. It will be deployed from a GAS (Get Away Special) canister that is located in the shuttle cargo bay. Between the two possible Hitchhiker designations, GAS and CAP (Complex Autonomous Payload) programs, PANSAT will most likely be designated as a CAP due to the need for a motorized door assembly and a launch mechanism [Ref. 1:p.2]. Figure 2 presents a pictorial of PANSAT's launch sequence as a member of the CAP program.

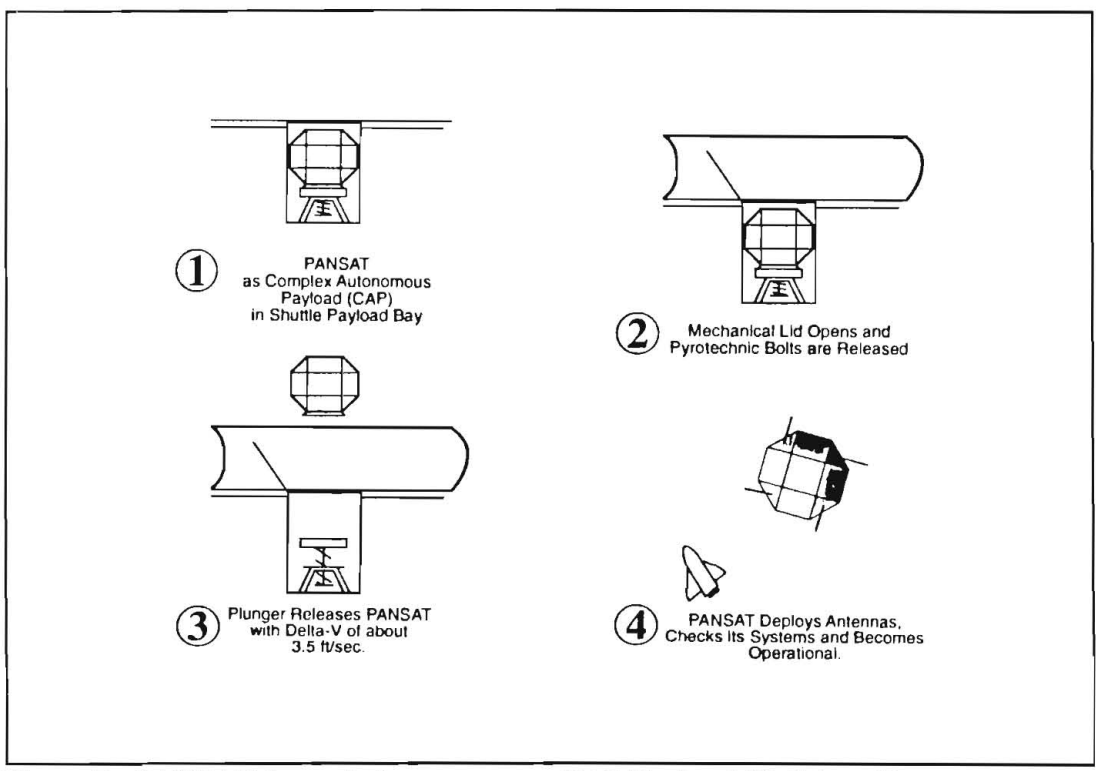

Figure 2. PANSAT Launch Sequence as a CAP Payload [Ref. 1:p. 2]

2. Space Shuttle Operations

To properly predict the lifetime and re-entry of PANSAT, it is imperative to understand the operating environment of the satellite. This includes the launch vehicle as well as the expected times of orbit insertion. As a member of the GAS program, PANSAT is considered as a secondary payload, and thus will have to accept the orbital elements that the primary payload demands.

The advertised limits of Space Shuttle operations are an altitude of between 110 nmi (203.7 km) and 330 nmi (611.2 km) with inclinations of 28.5^0 to 57.0^0 [Ref. 2]. The actual orbital elements for each mission depends on the mass of the payload carried as well as the number of orbital maneuvering system kits added to the Shuttle. This dependence is illustrated in Figure 3.

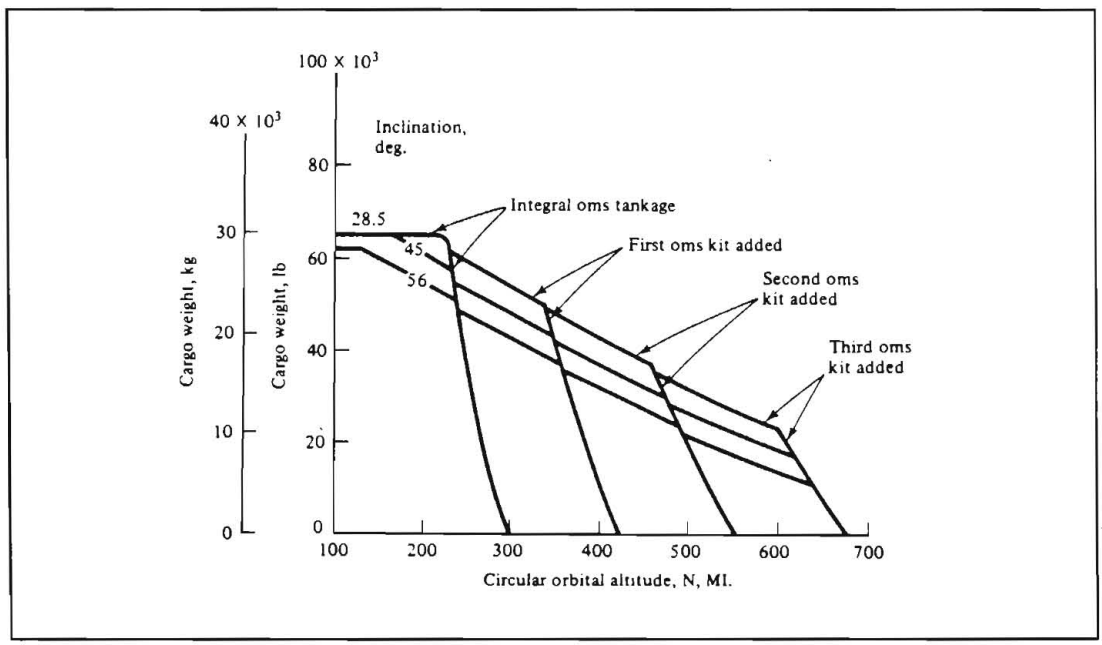

Figure 3. Space Shuttle Payload Performance to Circular Orbit [Ref. 3:p. 27]

According to NASA's internal planning documents [Ref. 4], 65 % of shuttle flights starting in late 1997 will be for assembling of the international space station. Table 1 provides the expected missions for the shuttle for 1996 through 1998. These dates are not firm, but will allow some planning for PANSAT orbital lifetime and re-entry. The altitudes and inclinations for STS-89 through STS-99 have not yet been determined due to those missions being so far in advance. Therefore, the altitude and inclination values in Table 1, from STS- 89 through STS-99, are estimated values taken from expected missions. The space station is expected to orbit from 180 nmi (333 km) to 240 nmi (444 km) above the Earth at 28.5^0 inclination [Ref. 5:p. 2-1]. Therefore, for the purpose of studies carried out in this thesis, all space station assembly and utilization flights were given default values of 220 nmi (407.4 km) with an inclination of 28.5^0.

TABLE 1. PROJECTED SPACE SHUTTLE MISSIONS

Flight	Orbiter	Launch Date	Payload or Objective	Altitude (nmi)	Altitude (km)	Inclination
STS - 76	Columbia	02-15-96	Tethered Satellite	160	296.3	28. 5
STS - 77	Atlantis	03-21-96	Mir Flight 3	213	394.5	51.6
STS - 78	Endeavour	05-02-96	Relay Satellite	160	296.3	28. 5
STS - 79	Discovery	06-27-96	Mir Flight 4	170	314.8	28. 5
STS - 80	Columbia	07-25-96	Spacehab 5	213	394.5	51.6
STS - 81	Atlantis	09-06-96	Mir Flight 5 / SPAS	213	394.5	51.6
STS - 82	Discovery	11-07-96	Mir Flight 6	160	296.3	28. 5
STS - 83	Columbia	12-05-96	Spacehab 6 / Spartan	213	394.5	51.6
STS - 84	Atlantis	01-30-97	Mir Flight 7	213	394.5	51.6
STS - 85	Endeavour	03-27-97	Hubble Serv. Flight 2	145	268.5	28.5
STS - 86	Discovery	04-17-97	Mir Flight 8	190	351.9	28.5
STS - 87	Columbia	05-30-97	Materials Sci. Lab. 1	213	394.5	51.6
STS - 88	Atlantis	06-26-97	Mir Flight 9	310	574.1	28.5
STS - 89	Endeavour	07-31-97	U.S. Microgravity	220	407.4	28.5
STS - 90	Discovery	10-02-97	Mir Flight 10	213	394.5	28.5
STS - 91	Endeavour	12-04-97	Space Station Ass. 1	220	407.4	28.5
STS - 92	Columbia	01-15-98	Space Life Sci. Flt. 4	213	394.5	51.6
STS - 93	Discovery	02-26-98	Space Station Ass. 2	220	407.4	28.5
STS - 94	Columbia	05-29-98	Spacehab 4	213	394.5	51.6
STS - 95	Endeavour	06-25-98	Space Station Ass. 3	220	407.4	28.5
STS - 96	Atlantis	07-30-98	Space Station Ass. 4	220	407.4	28.5
STS - 97	Discovery	09-24-98	Space Station Ass. 5	220	407.4	28.5
STS - 98	Endeavour	10-29-98	Space Station Util. 1	220	407.4	28.5
STS - 99	Atlantis	12-03-98	Space Station Ass. 6	220	407.4	28.5

C. PURPOSE OF STUDY

The focus of this thesis is to study and analyze the expected lifetime and reentry of PANSAT. Predicting the lifetime will allow designers an opportunity to schedule any experiments or specific events that must be completed prior to the satellite re-entering the Earth's atmosphere and being destroyed. Since PANSAT is not provided with a propulsion system for orbit sustenance, it is important to be able to predict orbit lifetime.

To aid in the prediction, a computer program, LIFETIME 4.1 was utilized. The program was developed by the Aerospace Corporation [Ref. 6], and allows customer inputs of orbital parameters, solar flux index, geomagnetic index, and ballistic coefficients along with the choice of atmospheric models and perturbations to be used. With the use of this program, along with the expected or predicted values of solar flux and geomagnetic indexes, a reasonably accurate prediction of PANSAT lifetime and reentry is possible to aid in the proper planning and operation of the satellite.

The following chapters provide the reader a detailed analysis of PANSAT orbitology. Chapter II provides an overview of satellite motion, orbital parameters, and the many phenomena that affect satellite lifetime such as atmospheric drag, solar pressure and the magnetic field of the earth. Chapter III introduces the LIFETIME 4.1 program and the equations used to predict PANSAT's life span and reentry. Chapter IV provides an detailed analysis of the program inputs and results and Chapter V predicts PANSAT's survivability from reentry. Chapter VI presents the conclusions.

II. OVERVIEW

A. INTRODUCTION

To provide a basic understanding of PANSAT lifetime and reentry, it may prove useful to briefly explain the environment and orbital parameters that will affect the satellite. This entails a brief introduction of the equations of motion, perturbations, and the diverse forces that determine the satellite's movement.

B. ORBITAL FUNDAMENTALS

1. Satellite Equations of Motion

To introduce the reader to the equations of motion governing satellite movement, a brief description of classical orbital elements is required. The classical method, known as the '2-body equations of motion' are based on Isaac Newton's mathematical approach of analyzing satellite orbits. Newton's 2nd Law of Motion, $\Sigma F=m\mathbf{a}$[1], applied to a constant mass system, combined with Newton's Law of Universal Gravitation, $F=-GMm/\mathbf{r}^2$[2], provide the necessary base to build orbital equations. Since PANSAT is a low-orbit satellite, gravitational effects of other celestial bodies may be neglected due to the extremely small perturbations they impose on the satellite orbit. Szebehely [Ref. 7:p. 131] states that if the altitude of a satellite is below 1600 km, the solar and lunar effects

---

[1] Where ΣF is the vector sum of all forces acting on the mass m and **a** is the vector acceleration of the mass measured relative to an inertial reference frame.

[2] Where F is the force on mass m due to mass M and **r** is the vector from M to m. The universal gravitational constant, G, has the value 6.67×10^{-11} Nm^2/kg^2.

(the so-called third body effects) may be neglected. An assumption necessary regarding the 2-body model is that both bodies are treated as though their masses are concentrated at their centers, known as 'point masses'.

When solving these 2-body equations of motion, 5 constants and one variable as a function of time are required. These 6 parameters, known as 'classical orbital elements' [Ref. 7] are defined below and are depicted in Figure 4.

a: semi-major axis: constant defining the size of the ellipse;

e: eccentricity: constant defining the shape of the ellipse;

i: inclination: the angle between the Earth's equatorial plane and the satellite's orbital plane;

Ω: right ascension of ascending node: the angle from the Vernal Equinox to the ascending node, the point where the satellite passes through the equatorial plane moving in a northerly direction;

ω: argument of perigee: the angle, in the plane of the satellites orbit, between the ascending node and the periapsis point, measured in the direction of the satellite's motion;

f: true anomaly: angle form the eccentricity vector to the satellite position vector, measured in the direction of satellite motion;

Alternatively, instead of using the true anomaly, it is possible to use T, time of periapsis passage: the time when the satellite was at periapsis.

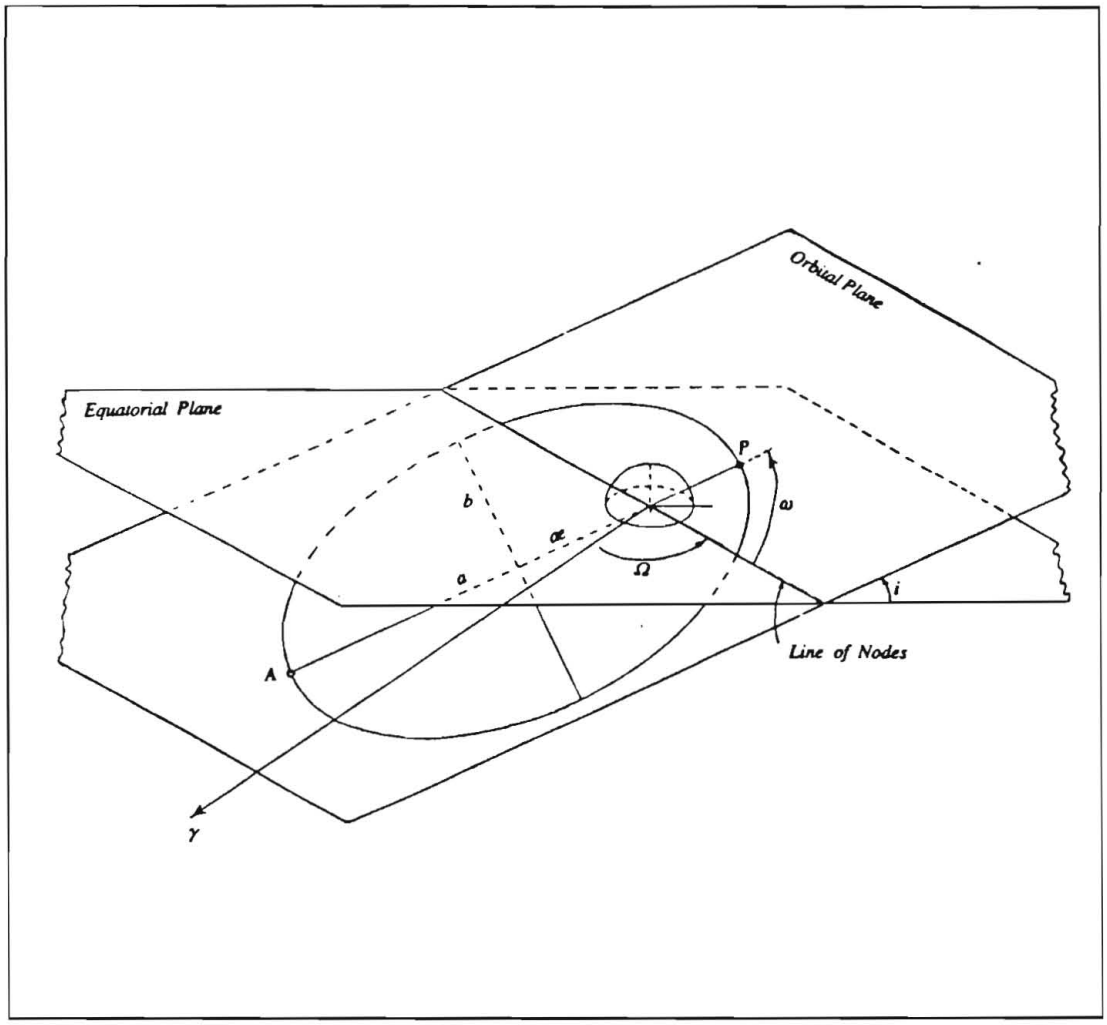

Figure 4. Orbital Elements [Ref. 7:p. 98]

There are many variables that will affect PANSAT's orbital lifetime. These include the altitude of orbit injection, atmospheric drag and density, the geomagnetic field of the Earth and the solar flux. Since the above items are exceptionally hard to predict or model, the following generic orbital equations can be used to approximate PANSAT's orbital characteristics [Ref. 8]:

circular velocity (km/s) $$V = \sqrt{\frac{\mu}{r}} = 631.3481 r^{-\frac{1}{2}} \quad (1)$$

period (min) $$P = 1.658669 x 10^{-4} r^{\frac{3}{2}} \quad (2)$$

revolutions per day (#) $$number = \frac{1436.07}{P} \quad (3)$$

maximum eclipse (min) $$time = \frac{a \sin(6378 / r)}{180^{O}} P \quad (4)$$

node precession rate (deg/day) $$number = -2.06474 x 10^{14} r^{-\frac{7}{2}} \cos \iota \quad (5)$$

where μ is the gravitational parameter of the earth (μ = 398601.2 km^3/sec^2) and r is the distance of the satellite from the center of the earth.

Table 2 provides a breakdown of expected PANSAT orbital characteristics for Space Shuttle altitudes. All calculations are done assuming a circular orbit utilizing equations (1) through (5).

C. SATELLITE ENVIRONMENT

1. Introduction

The growing importance on space operations and the increasing dependence on satellites has highlighted many geophysical problems. Phenomenon such as spacecraft charging, variations in drag, changes in solar activity, variations in the geomagnetic fields, and other occurrences, which were once ignored or neglected, must now be taken into account in order to predict a satellite's effectiveness and lifetime. A brief description of the major components that will affect PANSAT's lifetime is provided.

TABLE 2. PANSAT ORBITAL CHARACTERISTICS

Altitude (km)	Circular Velocity (km/s)	Period (min)	Revolutions per Day (#)	Maximum Eclipse (min)	Node Precession Rate (deg/day)
300	7.726	90.52	15.91	36.6	-8.48 cos i
350	7.697	91.54	15.73	36.3	-8.26 cos i
400	7.669	92.56	15.56	36.1	-8.05 cos i
450	7.640	93.59	15.39	35.9	-7.85 cos i
500	7.613	94.62	15.22	35.8	-7.65 cos i
550	7.585	95.65	15.05	35.6	-7.46 cos i
600	7.558	96.69	14.89	35.5	-7.27 cos i
650	7.531	97.73	14.73	35.4	-7.09 cos i
700	7.504	98.77	14.58	35.3	-6.92 cos i

These parameters are also included in the LIFETIME 4.1 program and are taken into account in the prediction of the satellite's life span.

2. The Earth's Atmosphere

The International Union of Geodesy and Geophysics at its 1951 Brussels meeting recommended the nomenclature summarized in Figure 5 for classifying the structure of the Earth's atmosphere [Ref. 9:p.278].

The troposphere, stratosphere, mesosphere, thermosphere, and exosphere are classified on a thermal basis. If the classification is by chemical composition, the main regions are the homosphere and heterosphere. The structure of the atmosphere can in addition be classified from a number of other viewpoints such as degree of ionization [Ref. 9: p.278].

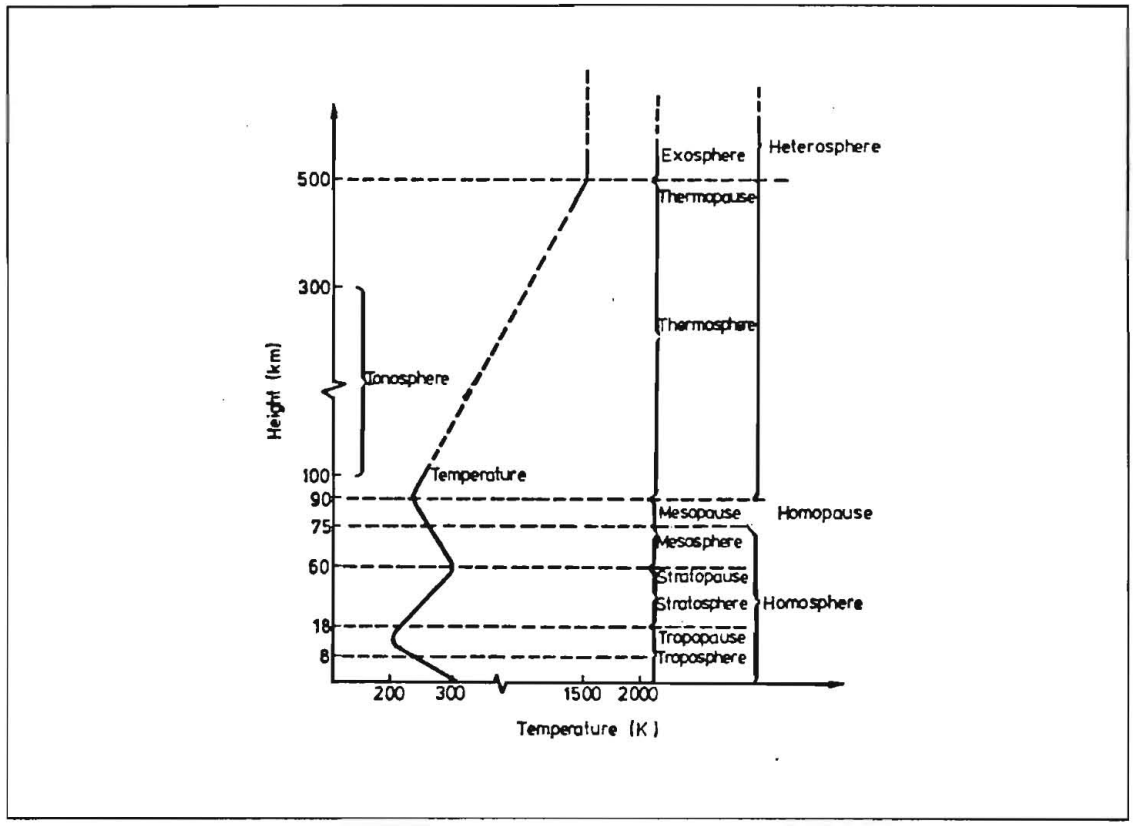

Figure 5. Structural Breakdown of Earth's Atmosphere [Ref. 9:p. 278]

Since PANSAT will operate anywhere between 268 and 575 km (see Table 1), the main area of interest will be the thermosphere. The thermosphere is a region above approximately 90 km where absorption of the sun's extreme ultra violet (EUV) radiation results in significant increases in temperature with altitude [Ref. 8:p.208]. Also, the thermosphere may be heated from geomagnetic activity and certain chemical reactions. At approximately 250 km, the temperature approaches a limiting value which ranges between 600 and 1200 K over the typical solar cycle and may reach as high as 1500 K. The solar and geomagnetic influence is extremely variable and notably difficult to predict.

Heating of the thermosphere increases atmospheric density because the thermosphere's expansion causes increased pressure in the atmosphere [Ref. 8:p. 208].

3. Solar Physics

Although the Sun is only one of about 10^{11} stars in our galaxy, its importance to life on Earth is apparent. However, it is only of recent that its significance to satellite lifetime has been observed. The amount of its effect depends on whether the Sun is "quiet" or "active". A "quiet sun" represents the total background output which has been studied and classified as 'blackbody' emissions. The nominal value is approximately 1358 $\pm$ 5W/m^2 [Ref. 8:p. 410] measured at 1 astronautical unit (AU) or 93 million miles.

Discrete localized surface sources are qualities of an 'active sun'. Considered a gaseous body, the sun does not rotate like a rigid bodied planet. Due to this differential rotation between the sun's equator (24.9 days) and poles (31.5 days), it is believed that the sun's magnetic field becomes twisted and concentrated into distinct regions. The release of this built up magnetic energy takes the forms of solar flares, sunspots and prominences. A solar flare is a highly concentrated explosive release of energy within the solar atmosphere which appears as a sudden, short-lived brightening of a localized area in the chromosphere. Flares are classified according to their size and intensity based on the fraction (in millionths) of the solar disk. Sunspots are the most commonly reported solar activity and are thought to be regions of very strong magnetic fields on the order of several thousand gauss [Ref. 10:p. 15-18].

The Sun emits huge amounts of energy and mass which dramatically affects Earth's atmosphere. This effect follows a cycle known as the 'solar cycle'. Recent analysis have shown the average period length is about 11 years, with a spread of periods from 7 to 13 years. Each cycle is defined as beginning with solar minimum and lasting until the following solar minimum. The typical cycle takes 4 years to rise from a minimum to a maximum and about 7 years to fall back to minimum [Ref. 10:p. 19].

Solar cycle minimum and maximum is characterized by the number of sunspots and the intensity of solar flares observed. During solar maximum, daily sunspot numbers can normally be over 100 while several consecutive days of a zero reading are possible during a solar minimum. Table 3 provides observed and expected sunspot activity.[Ref. 8:p. 203]

TABLE 3. YEARS OF SOLAR CYCLES 21-25

Solar Cycle	21	22	23	24	25
Sunspot Maximum	1979	1990	2001	2012	2023
Sunspot Minimum	1985	1996	2007	2018	2029

4. F10.7

According to Tascione [Ref. 10:p. 61], the Sun's EUV output imitates a pattern similar to the sunspot number, and this fluctuation translates into a variation of energy available to the thermosphere. The subsequent variation in temperature, in turn, produces a solar cycle variation of atmospheric density. Although EUV flux observations have rarely been made since ozone absorbs nearly 100% of incoming EUV radiation, we can infer the value based an 2.8 GHz solar radio flux measurements because EUV and 2.8

GHz fluxes show a fairly good correlation. The 2800 MHz flux is better known as the 10.7 cm flux or as F10.7.

Daily values of F10.7 are measured in Penticton, Canada with a 2000Z reading accepted as the world daily standard [Ref. 11:p. 21]. As previously noted, these values themselves have no significant impact on the atmosphere but are representative of the EUV radiation that heats the thermosphere. Measured in units of 10^{-22} W/(m^2*Hz), extreme values of F10.7 range from 50 to 250, with an average index reading between 70 and 225 [Ref. 8:p. 212].

Figure 6 gives chronicled solar activity data by plotting the mean monthly F10.7 index of radio flux from the Sun. The peaks in the F10.7 index coincide very nearly to solar maxima, to levels of high solar activity, and consequently, to levels of high atmospheric density. Notice that the variations are considerable on a month-to-month basis and that one solar maximum may have levels that differ dramatically from other solar maxima. Accordingly, predicting the solar flux is not yet accurate although, the predicted average value over an extended period is computable [Ref. 8:p. 208].

5. Magnetic Index - Ap

Magnetic disturbances, sometimes called magnetic storms, play an important role in satellite lifetime. Magnetic variations differ in character and intensity depending on latitude, and records have shown that sometimes magnetic disturbances reappear with the 27 day average rotation rate of the Sun [Ref. 10:p. 40].

The *K* index (magnetic index) is a 3 hour interval measurement of the irregular

variations of standard magnetic field measurements and is use as an indicator of the general level of magnetic activity caused by the solar wind [Ref. 10:p. 40]. This index has a range of 0 to 9, and is measured on a quasi-logarithmic scale.

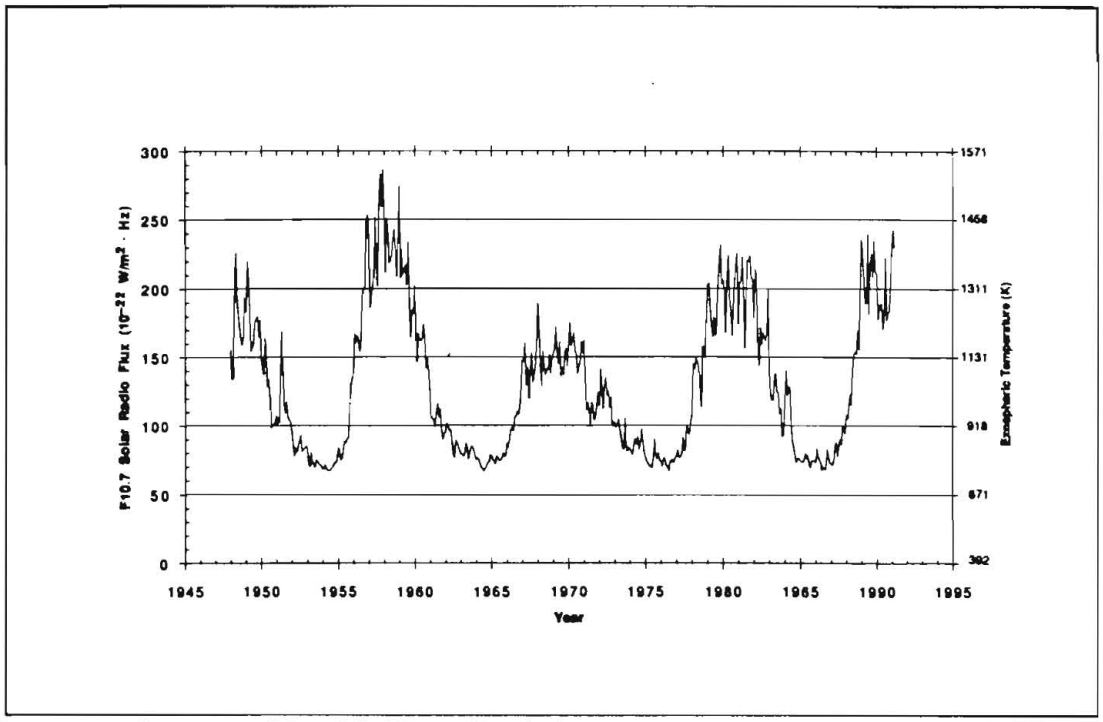

Figure 6. Observed Monthly Mean Radio Flux at 10.7 cm [Ref. 8:p. 209].

The *Kp* index ('p' for planetary) is based on the *K* indices from twelve worldwide stations between geomagnetic latitudes of 48^0 and 63^0. Values of *K* are first used to filter out the local and seasonal variables resulting in *Ks* values of finer gradations, with the *Kp* values derived from *Ks* index. To allow daily averaging of the indices, the *K* indices are converted to a linear scale called the A indices [Ref. 10:p. 40].

The linearization is provided below:

Kp	0_0	0_+	1-	1_0	1_+	2-	2_0	2_+	3-	3_0	3_+	4-	4_0	4_+	5-	5_0	5_+	6-	6_0	6_+	7-	7_0	7_+	8-	8_0	8_+	9-	9_0
Ap	0	2	3	4	5	6	7	9	12	15	18	22	27	32	39	48	56	67	80	94	111	132	154	179	207	236	300	400

The planetary daily average of Ap is computed by averaging the a_p values over a 24 hour period [Ref. 11:p. 23]

$$Ap = \sum_{i=1}^{8} \frac{a_{pi}}{8} \tag{6}$$

This daily average, usually between 4 and 70 nT, is an entered value for Lifetime 4.1.

6. Atmospheric Density

Although the overall behavior of atmospheric density is well established, exact properties are difficult to ascertain and are highly variable. Because there are many diverse physical processes that occur in the thermosphere, there are various methods used in calculating the atmospheric density.

A basic relation used in many models is the hydrostatic relationship. In differential form, the relation is

$$dp = -\rho g dr \tag{7}$$

where p = atmospheric pressure;

g = acceleration due to gravity; and

ρ = density.

Equation (7) above can also be written as

$$\frac{dp}{p} = -\frac{mg}{kT} dr = -\frac{1}{H} dr \tag{8}$$

where m = average particle mass;

T = absolute temperature at height r;

k = Boltzman constant; and

H = scale height.

By integrating (8), neglecting the variation of g with altitude, and realizing density is proportional to pressure via the perfect gas law, the result is the exponential function

$$\rho = \rho_0 e^{\frac{-(r-r_o)}{H}} \tag{9}$$

As can bee seen from equation (9), density is a function of temperature and, as stated earlier, temperature is affected by F10.7. Figure 7 provides the atmospheric density as a function of altitude corresponding to various values of the F10.7 index. As can be seen from the figure, densities below about 150 km are not dramatically affected by solar activity. However, inspection between the altitudes of 500 to 800 km reveal that the density variations between solar maximum and minimum are roughly two orders of magnitude [Ref. 8:p. 208].

Air density also exhibits a day-to-night rhythm, known as diurnal variations, reaching a maximum about 2 hours after midday and a minimum between midnight and dawn. At a height of 600 km, the maximum daytime density may be 8 times as greater than the nighttime minimum. Other variations are caused by the 27 day rotational period of the sun. [Ref. 12:p.258]

LIFETIME 4.1 has the option of using either the Jacchia/Walker 64 atmospheric model or the Jacchia 71 model. The program suggests that the Jacchia/Walker 64 model be used for satellite altitudes below 90 km, and the Jacchia 71 model for altitudes 90 km and above. Since the proposed PANSAT altitude is shuttle dependent, the Jacchia 71

model was selected for orbit analysis. This model takes into account the values of F10.7 and Ap to calculate density as a function of altitude and temperature.

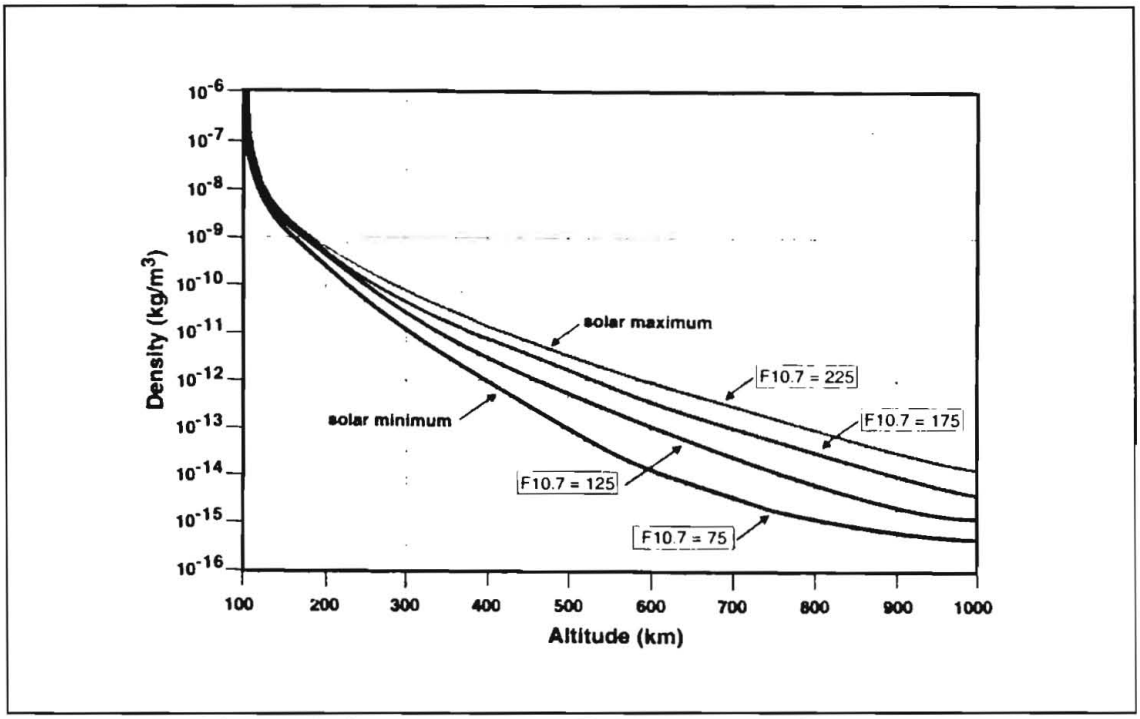

Figure 7. Density vs. Altitude for Various F10.7 Values [Ref. 8:p. 209].

7. Coefficient of Drag

The coefficient of drag, C_D, is in itself an extremely difficult quantity to obtain. In order to obtain the correct coefficient of drag, an analysis must be conducted on the interaction of atmospheric molecules with the surface of the spacecraft. The value of the drag coefficient C_D depends on the shape of the vehicle its attitude with respect to the velocity vector, and whether it is spinning, tumbling or stabilized [Ref. 12:p. 258].

The coefficient of drag also strongly depends whether or not the satellite is in a continuum or in a free-molecular flow. The airflow around the spacecraft can be

determined by looking at the ratio of the mean free path of the atmospheric molecules to the characteristic linear dimension of the moving body. When this number, known as the Knudsen number, is much greater than unity, free-molecular flow prevails; when the ratio is smaller than unity, a continuum aerodynamic regime exists, and the coefficient of drag is less than half the value of the free-molecular flow value. All satellites above 200 km are considered to be in free-molecular flow. [Ref. 13]

The determination of the coefficient of drag for any given body is quite difficult. For spacecraft above 200 km, it is conventional to use a coefficient of 2.2 for a spherical body, and a coefficient of 3.0 for a cylindrical body. [Ref. 8:p. 258]

8. Ballistic Coefficient

The ballistic coefficient is simply the "mass quantity" divided by the "drag quantity". The more "massive" an object and/or the smaller the drag, the greater the value of the ballistic coefficient. Objects with high ballistic coefficients tend to be less affected by passage through the atmosphere. [Ref. 12:p. 258]

The ballistic coefficient is defined as

$$B = \frac{M}{C_D A} \tag{10}$$

where M = mass of the satellite;

C_D = coefficient of drag; and

A = cross-sectional area of the spacecraft.

The value of the ballistic coefficient B can either be estimated or bound by upper and lower limits if a variation in any of the quantities is anticipated. In some instances, uncertainties in predicting atmospheric models may be absorbed in the calculation of this parameter. LIFETIME 4.1 attempts this by providing differential corrections for the ballistic coefficient through a simple least squares procedure using the semi-major axis, a, and the eccentricity, e, as observable inputs.

9. Atmospheric Drag

Due to the growing importance of satellite lifetime prediction, several atmospheric models, or satellites drag models, have been developed and are currently used for practical applications such as lifetime estimates, reentry prediction, orbit determination and tracking, attitude dynamics, and most recently, mass analysis of a particular satellite. Besides LIFETIME 4.1, upon which this thesis work is based, other programs such as Orbital Workbench by Cygnus Engineering and SATRAK, developed by Headquarters, Air Force Space Command, serve as a satellite orbital propagator and analysis tools.

Atmospheric drag affects all low-earth-orbit satellites with an orbit perigee height below 1000 km. It is a nonconservative force with a cumulative effect of removing energy from the satellite's orbit. As energy is removed, the orbit contracts causing an increase in the forces acting on the satellite. As the orbit contracts, the semi-major axis and period decrease. However, to satisfy Kepler's 3rd Law ($\mu = n^2a^3$ = constant), the orbit velocity is increased [Ref. 12:p. 213]. The net result is referred to by Chobotov [Ref. 12] as a

"drag paradox": the effect of atmospheric friction is to speed up the motion of the satellite as it spirals inward.

Another effect of air drag is that an elliptical orbit becomes circular. This occurs because air drag is much more prominent at perigee, the point where the satellite is at its lowest altitude. Since the velocity and atmospheric density are greatest at perigee, the energy drain is also the greatest at this point. The energy drain causes the satellite to slow, resulting in the lowering of the apogee height. This cycle continues until the apogee height is equal to the perigee height at which point the elliptical orbit becomes circular and, eventually, the satellite will reenter the atmosphere. A pictorial presentation of the effects of atmospheric drag on an elliptical orbit is shown in Figure 8.

Atmospheric drag can be considered a tangential force and acts opposite the velocity vector. The following equation is used to represent the atmospheric drag acceleration which is placed on an orbiting body:

$$a_D = \tfrac{1}{2} C_D \frac{A}{M} \rho V^2 \qquad (11)$$

where a_D is the drag acceleration exerted on the satellite, C_D is the coefficient of drag of the satellite, A is the cross sectional area of the satellite perpendicular to the direction of motion, M is the satellite mass, V is the satellite velocity relative to the atmosphere, and ρ is the local atmospheric density. For an accurate velocity estimate of a satellite, it is necessary to combine the geocentric velocity of the satellite, the contribution due to earth rotation, called precession, and the wind contribution which is at times quite significant depending on altitude. The quantities C_D, A, and M constitute the ballistic coefficient.

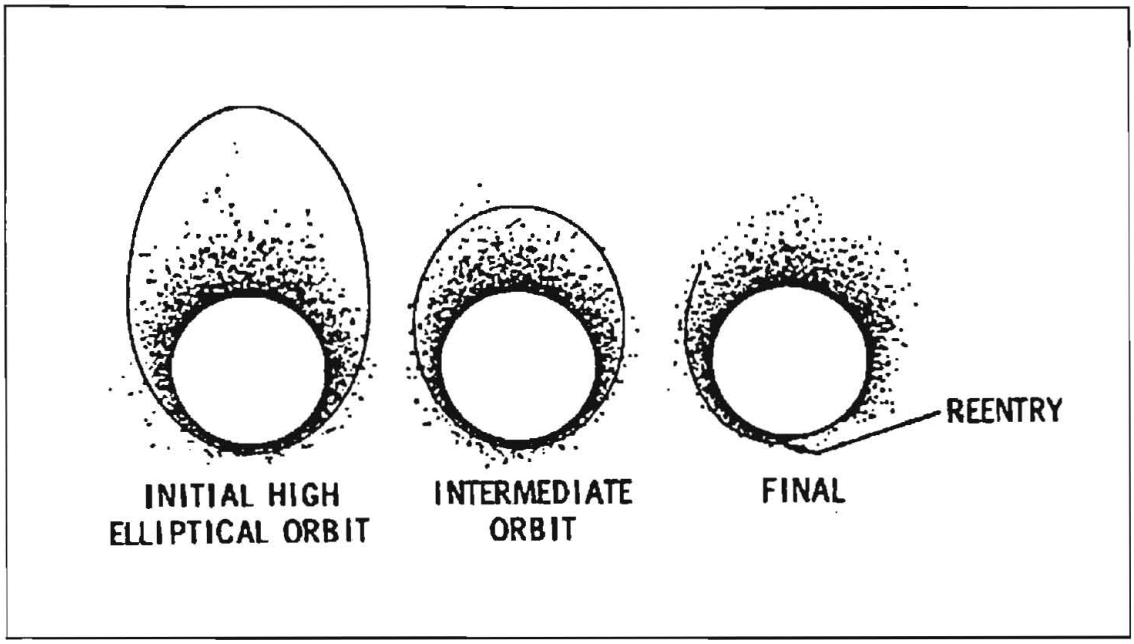

Figure 8. Drag Effects on High Eccentricity Orbits [Ref. 14:p. 27]

Since PANSAT will be inserted into a circular orbit, changes in altitude, orbital period, velocity and eccentricity per revolution can be approximated by the following equations [Ref. 8:p. 143]:

$$\Delta a_{rev} = -2\pi B\rho a^2 \tag{11}$$

$$\Delta P_{rev} = -6\pi^2 B\rho a^2/V \tag{12}$$

$$\Delta V_{rev} = \pi B\rho aV \tag{13}$$

$$\Delta e_{rev} = 0 \tag{14}$$

A considerably more accurate estimate, although still approximate, is obtained by integrating equation.(10), taking into account the changes in atmospheric density with both altitude and solar activity. This integration is done by the LIFETIME 4.1 program.

Table 4, taken from Larson and Wertz [Ref. 8], provides atmospheric and orbital decay information taken from the Mass-Spectometer-Incoherent-Scattter-1986 (MSIS86) Neutral Atmospheric Model. The atmospheric density information includes an F10.7 index of 120 for the mean values and a 220 index for the maximum density which is representative of high solar activity. The orbital decay rates are calculated for a satellite of PANSAT's characteristics.

TABLE 4. PANSAT ENVIRONMENT AND DECAY BASED ON MSIS 86

Altitude (km)	Atmo-spheric Scale Height (km)	Atm. Density Mean (kg/m^3)	Atm. Density Maximum (kg/m^3)	Orbital Decay Rate Mean (km/yr)	Orbital Decay Rate Maximum (km/yr)
300	50.3	1.87×10^{-11}	4.84×10^{-11}	-1.73×10^{2}	-4.47×10^{2}
350	54.8	6.66×10^{-12}	2.18×10^{-11}	-6.22×10^{1}	-2.02×10^{2}
400	58.2	2.62×10^{-12}	1.05×10^{-11}	-2.43×10^{1}	-9.76×10^{1}
450	61.3	1.09×10^{-12}	5.35×10^{-12}	-1.02×10^{1}	-4.99×10^{1}
500	64.5	4.76×10^{-13}	2.82×10^{-12}	-4.46×10^{0}	-2.64×10^{1}
550	68.7	2.14×10^{-13}	1.53×10^{-12}	-2.01×10^{0}	-1.44×10^{1}
600	74.8	9.89×10^{-14}	8.46×10^{-13}	-0.93×10^{0}	-7.98×10^{0}
650	84.4	4.73×10^{-14}	4.77×10^{-13}	-0.45×10^{0}	-4.51×10^{0}
700	99.3	2.36×10^{-14}	2.73×10^{-13}	-0.22×10^{0}	-2.59×10^{0}

10. Zonal Harmonics

Zonal harmonics, or Earth gravity harmonics, are derived from the gravity potential theory. This accounts for a non-spherical Earth with the most dominant features of an equatorial bulge, a slight pear shape, and a flattening at the poles. The effects of these harmonics depend on latitude and are known as dimensionless geopotential

coefficients, J_n, where n represents the harmonic term. The potential created by a non-spherical Earth cause periodic variations in all of the orbital elements. The most commonly encountered and dominant harmonic is the J_2 harmonic which represents the Earth's equatorial oblateness. The J_2 term causes secular variations in the right ascension of ascending node and the argument of perigee. These rates can be computed by the following equations [Ref. 8:p. 141]:

$$\Omega_{J_2} = -\frac{3}{2} n J_2 \left(\frac{R_E}{a}\right)^2 (\cos i)\left(1-e^2\right)^{-2} \tag{15}$$

$$\omega_{J_2} = \frac{3}{2} n J_2 \left(\frac{R_E}{a}\right)^2 \left(4-5\sin^2 i\right)\left(1-e^2\right)^{-2} \tag{16}$$

where n = the mean motion in deg/day, R_E is the radius of the Earth, and the rest of the quantities are as defined on page 9.

The J_3 harmonic term is due to the polar bulge and is on the order of 10^{-3} J_2 for the Earth, so that the amplitudes of the short-period perturbations will be very small [Ref. 9:p.291]. However, amplitudes of long period variations for eccentricity and inclination may reach a noticeable value.

Geometrical interpretations of the first two zonal harmonics, J_2 and J_3, are shown in Figure 9. The Earth's oblateness is represented by a combination of J_2 and the rotation of the Earth. The difference between the polar and the equatorial radii of the Earth is 21.4 km. The pear shape of the Earth is caused by J_3. The height of the bulge at the North Pole is about 16.5 m. Accepted values of J_2 and J_3 are provided.

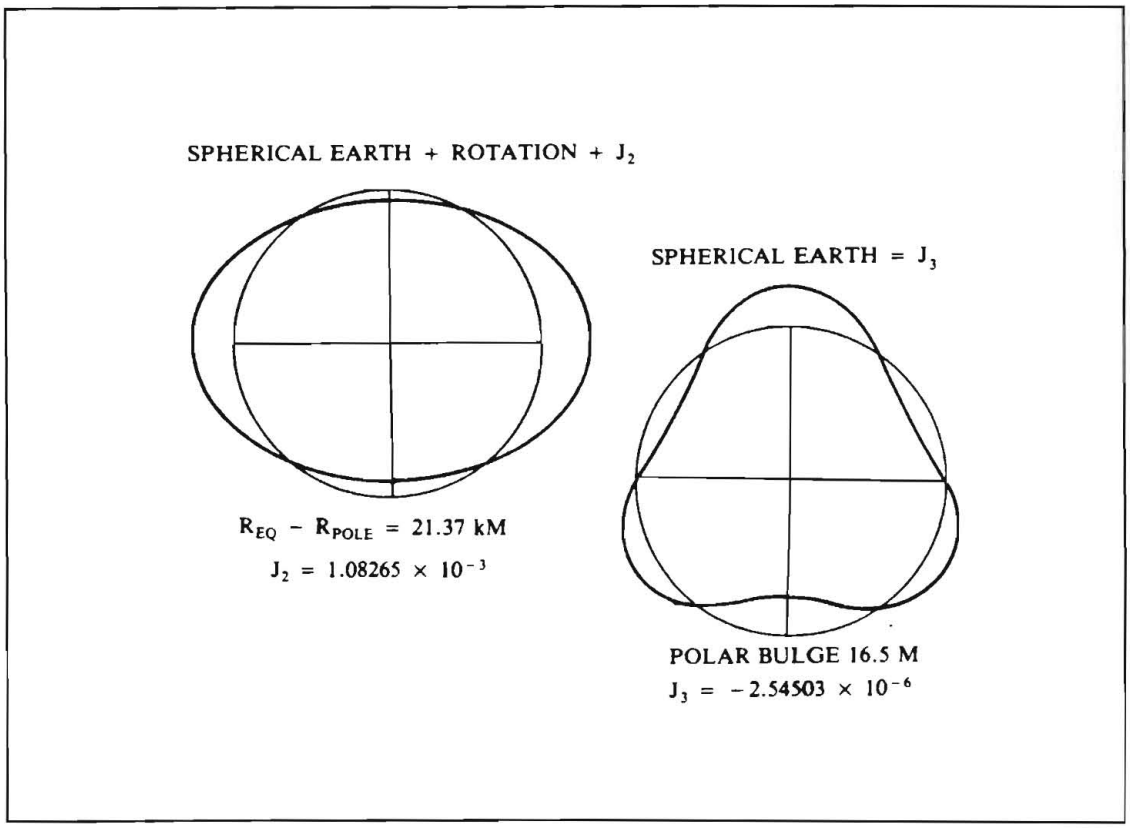

Figure 9. Earth's Zonal Harmonics [Ref. 12:p. 292]

11. Summary

As outlined in this chapter, many variables affect the environment of a satellite and hence, its life. This chapter attempted to provide a basic understanding of the importance these elements hold in predicting satellite motion and lifetime. Every topic covered in this chapter is also a optional input into LIFETIME 4.1 for PANSAT analysis.

III. LIFETIME 4.1

A. INTRODUCTION

LIFETIME 4.1, developed by Aerospace Corporation [Ref. 15], is an orbit propagating tool developed for use on IBM/PC *86 series and Macintosh computers to efficiently and accurately predict satellite orbit lifetimes. The analysis is based on simplified averaged equations of motion in classical orbital elements.

LIFETIME 4.1 is unique because it gives the user a wide variety of options to help in the analysis of orbit lifetime. The advertised capabilities of LIFETIME 4.1 include:

1. accurate prediction of orbit decay in a dynamic atmosphere that models the 11 year solar cycle (Jacchia 64 or 71 model);
2. orbit sustenance simulation and fuel requirement estimation;
3. differential corrections of the ballistic coefficient using observed orbit decay data;
4. allowing the solar arrays to follow the sun for an accurate prediction of the effective cross-sectional area as a function of time; and
5. generation of high quality plots on screen and on a laser printer.

Note that capabilities 3 and 4 are unique features of LIFETIME that should significantly improve the accuracy of a satellite's lifetime prediction over existing models. [Ref. 6:p.2]

B. PROGRAM DESCRIPTION

This section presents the formulation of the semianalytic theory which was simplified from the work of Liu and Alford [Ref. 16], and specially tailored by Chao, [Ref. 6], to

allow the program to run on a personal computer. This work includes integrating the averaged equations of motion with a step size of at least one orbit period. The Gaussian quadrature method of integration is used for the semi-major axis, eccentricity and atmospheric drag calculations and only the J_2 harmonic effect is used for computing the atmospheric density. [Ref. 15]

1. Simplified Semianalytic Theory

The following section is taken directly from [Ref. 6] to ensure completeness and accuracy:

The LIFETIME program utilizes the integration of the mean classical orbit elements to achieve accurate lifetime predictions. The following equations are simplified from Liu and Alford [Ref. 16] and are summarized:

$$\frac{da}{dt} = -\frac{1}{2\pi}\int_0^{2\pi} B\rho V\left(\frac{a}{1-e^2}\right)\left[1+e^2+2e\cdot\cos(f)-\omega_e\cdot\cos(i)\sqrt{\frac{a^3(1-e^2)^3}{\mu}}\right]dm \quad (17)$$

$$\frac{de}{dt} = -\frac{1}{2\pi}\int_0^{2\pi} B\rho V\left[e+\cos(f)-\frac{r^2\omega_e\cdot\cos(i)}{2\sqrt{\mu a(1-e)^2}}\left[2(e+\cos(f)-e\cdot\sin^2(f)\right]\right]dm$$
$$-\frac{3}{8}nJ_3\left(\frac{R_E}{p}\right)^3\sin(i)(4-5\sin^2(i))(1-e^2)\cos(\omega) \quad (18)$$

$$\frac{di}{dt} = 0 \quad (19)$$

$$\frac{d\Omega}{dt} = -\frac{3}{2}nJ_2\left(\frac{R_E}{p}\right)^2\cos(i) \quad (20)$$

$$\frac{d\omega}{dt} = \frac{3}{4}nJ_2\left(\frac{R_E}{p}\right)^2(4-5\sin^2(i))+\frac{3}{8}nJ_2\left(\frac{R_E}{p}\right)^3\times$$
$$\left[(4-5\sin^2(i))\frac{\sin^2 i-e^2\cos^2 i}{e\cdot\sin(i)}+2\sin(i)(13-15\sin^2 i)e\right]\sin(\omega) \quad (21)$$

The integration step size is in multiples of orbit period and

$B = C_D A/Ms$ (Ms = Satellite Mass);

$$V = \left[\frac{\mu}{p}(1+e^2+2e\cdot\cos(f))\right]^{\frac{1}{2}}\left[1-\frac{(1-e^2)^{\frac{3}{2}}}{1+e^2+2e\cdot\cos(f)}\frac{\omega_e}{n}\cos(i)\right] \quad (22)$$

Other variables listed above are:

B: inverse of ballistic coefficient
V: satellite velocity relative to the atmosphere
μ: Earth gravitational constant = 3.986012×10^5 km^3/sec^2
R_E: Earth equatorial radius
ω_e: Earth rotation rate
p: semi-latus rectum and is equal to $a(1-e^2)$
n: satellite orbit mean motion
ρ: atmosphere density
M: mean anomaly

The integrations, which give the averaged drag effects on a and e with respect to M from 0 to 2π, are carried out with respect to the true anomaly f through the transformation:

$$dM = \left(\frac{r}{a}\right)^2 \frac{1}{\sqrt{1-e^2}}df \quad (23)$$

The integrations in a and e for a given orbit are then computed by the Gaussian quadrature method. The variable ρ is the density of the atmosphere and is determined from the Jacchia-Walker analytical model or the Jacchia 1971 model through

$$\rho = \rho(h, \phi, t_L, F10.7, Ap)$$

where

$$h = r - R$$

and

t_L = local time of the satellite,
ϕ = geocentric latitude of the satellite,
F10.7 = solar flux index,
Ap = index of magnetic activity,
r = satellite geocentric radius, and
R = geocentric radius of the oblate Earth surface at the satellite geocentric subpoint.

The satellite radius r, is the sum of the mean radius and the short-period variation due to J_2.

$$r = \frac{a(1-e^2)}{1+e*\cos(f)} + \delta r \quad (24)$$

where

$$\delta r = J_2\frac{Re^2}{\rho}\left\{\frac{1}{4}\sin^2(i)\cos 2(\omega+f) - \left[\frac{1}{2}-\frac{3}{4}\sin^2(i)\right]*\left[1+\frac{e\cos(f)}{1+\sqrt{1-e^2}}+\frac{2}{\sqrt{1-e^2}}\frac{r}{a}\right]\right\} \quad (25)$$

A good approximation for the terrestrial surface considering the Earth flattening effect is

$$R = Re(1-f_E\sin^2\phi) \quad (26)$$

with

$$\sin \phi = \sin (i) \sin(\omega + f) \qquad (27)$$
$$f_E = 0.00335$$

Again, this entire section was copied from [Ref. 6] to explain the semianalytic theory used in LIFETIME calculations.

2. Reentry Prediction

Since PANSAT is not designed to return to Earth successfully, the problem of protection to survive reentry does not exist. However, accurate reentry predictions are important because of the possibility of debris impact that may cause property damage and casualties. One of the unique capabilities of LIFETIME is the ability to predict an impact point, known as a 'footprint'. LIFETIME incorporates an integration algorithm and breakup model to allow the user to analyze possibilities of survival and the potential areas where an impact may occur. A Runge-Kutta 7(8) numerical integration routine allows for propagation through a breakup region and down to impact. The breakup region has a default value of 77.8 km for aluminum and magnesium material satellites or allows the user to enter a different altitude depending on the type of material used in satellite construction. The semi-analytic propagation method previously described, carries the satellite to one step below the integration start altitude which has a default value of 125 km for aluminum structures or also allows the user to adjust this number manually depending on the material used. [Ref. 15]

When the orbit propagation carries the satellite one step below the integration start altitude, LIFETIME resets the orbital elements to the previous step and begins the

numerical integration procedure. The result is a satellite modeled through the breakup altitude with an impact footprint being computed. The footprint is defined between the 'heel' point, which is the latitude and longitude directly below the breakup altitude, and the 'toe' point, predicted by a hard-wired increase of the ballistic coefficient to account for low drag debris that may survive the breakup. Figure 10 illustrates the integration and breakup model of LIFETIME, and Figure 11 provides an illustration of a 'footprint'.

3. Program Accuracy

Many factors influence the accuracy of lifetime predictions of any satellite. Variations in accuracy will depend on [Ref. 6:p. 8]:

1. F10.7 and AP prediction accuracy;
2. Long-term and secular variations in ballistic coefficient;
3. Atmospheric model approximations;
4. Accuracy of NORAD observations and information;
5. Unmodeled spacecraft maneuvers.

As presented by Strizzi [Ref. 17:p. 20], the USAF Space Surveillance Center (SSC) sets an upper limit of 20 % as an acceptable value of error in it's Tracking and Impact Prediction (TIP) process. Aerospace Corporation has done significant studies using LIFETIME and actual observations of decayed satellites using NORAD data. The amount of error from this comparison ranged between 2 and 15 % with most prediction errors being well below 10 % [Ref. 15]. As part of this thesis, a separate analysis was done by researching decayed satellites that closely resembled PANSAT in terms of shape, mass and ballistic coefficient.

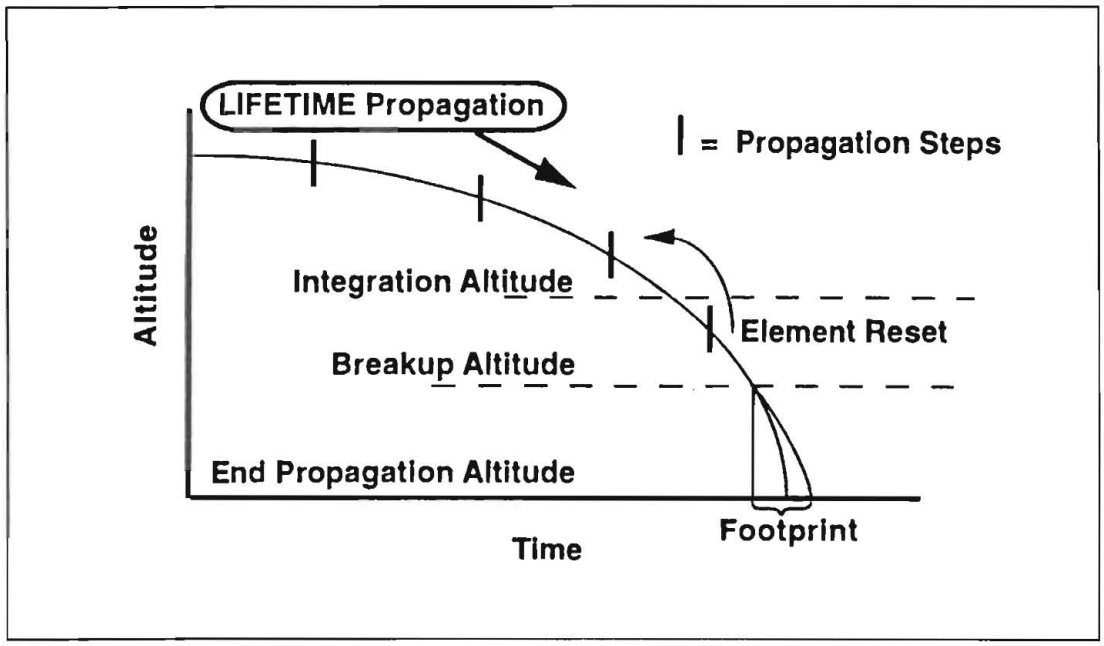

Figure 10. Illustration of Integration and Breakup Model [Ref. 15]

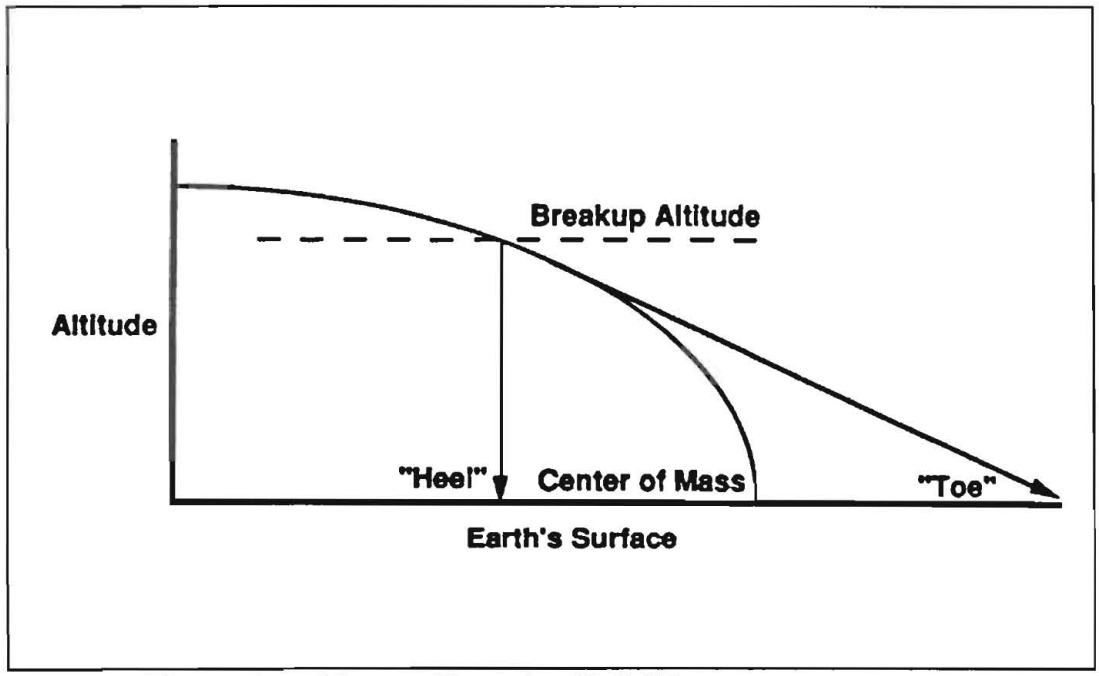

Figure 11. Illustration of Impact Footprint [Ref. 15]

The error from this separate study ranged between 8 and 10 %. Therefore, it is a reasonable assumption that LIFETIME predictions for PANSAT lifetime and reentry are accurate to within 10 %.

4. LIFETIME Output

As formerly noted, one of the unique features of LIFETIME is the ability to provide high resolution plots. Figure 12 shows the perigee/apogee decay history. Figure 13 gives the last revolution of the satellite on a world map. This figure also gives the expected latitude and longitude for the impact point for the center of mass. The start of the continuous (darker) ground trace is the breakup point with the segment between the triangles representing the predicted footprint of impact debris. Finally, Figure 14 shows the altitude history of the reentering satellite with predicted impact time (GMT) printed on the plot. All of these figures are representative of PANSAT at the extreme values of F10.7 and Ap at a starting altitude of 350 km. Note that the release point for PANSAT, the point where reentry begins, also affects the predicted impact point.

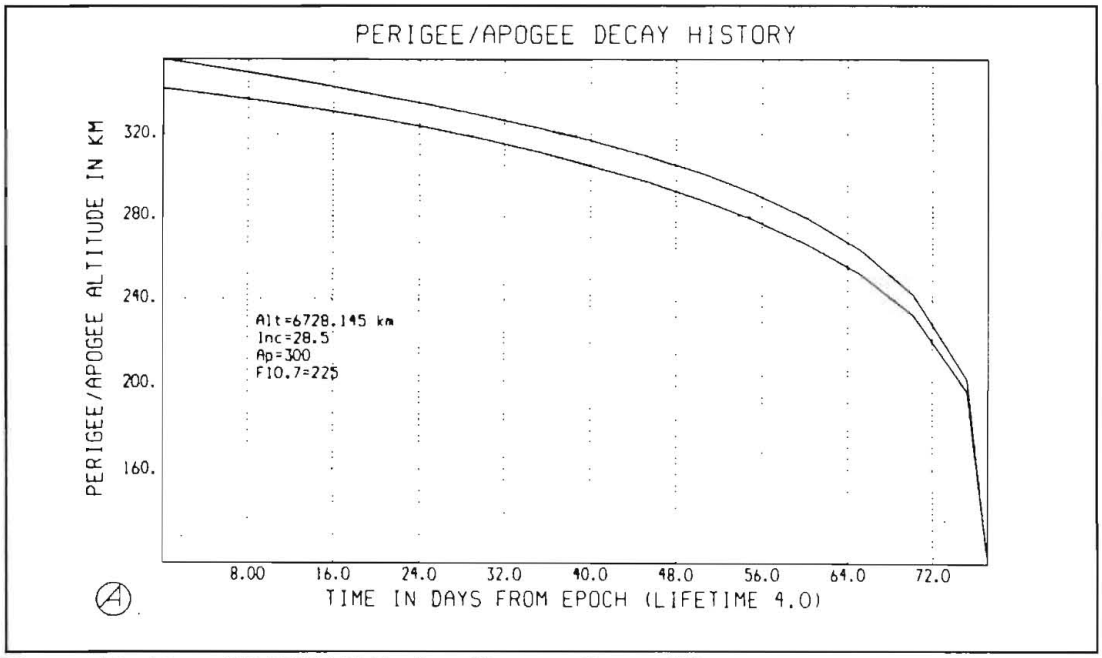

Figure 12. Plot of PANSAT Perigee/Apogee Decay History

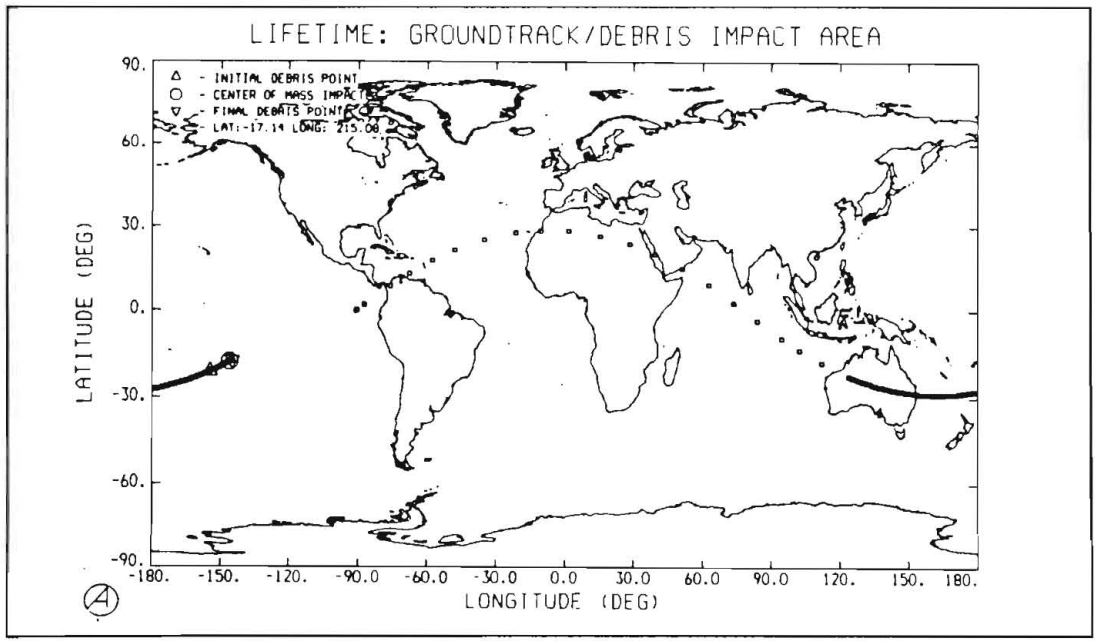

Figure 13. Groundtrack / Debris Impact Area

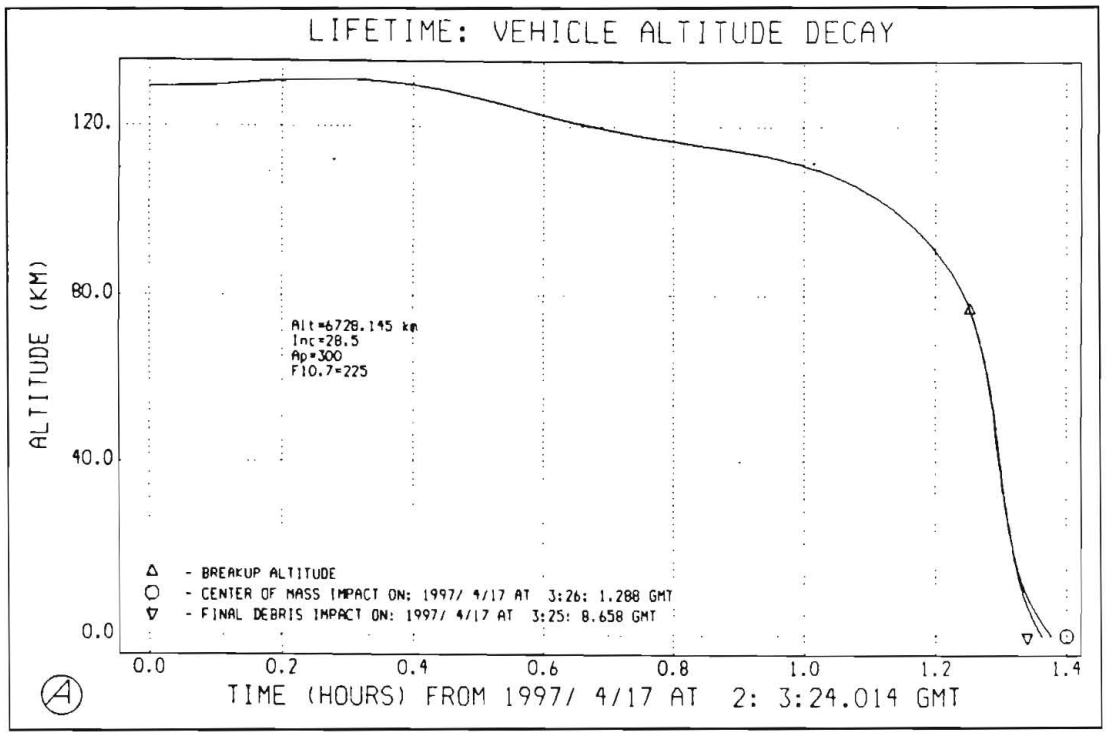

Figure 14. Vehicle Altitude Decay History

IV. RESULTS AND ANALYSIS

A. INTRODUCTION

LIFETIME supplies the user with up to 20 screens of data input depending on the options chosen. The basic procedure was to provide expected PANSAT insertion altitudes, inclinations and eccentricity depending on expected Space Shuttle missions, enter actual or assumed PANSAT data such as mass and ballistic coefficient, input predicted F10.7 and Ap data or use the built in default of an unbiased 11 year solar cycle, and finally provide the length of propagation, integration and breakup altitudes. The following is a breakdown in order of the assumptions and inputs provided to the LIFETIME program to aid in the analysis of PANSAT's orbital lifetime and reentry prediction.

B. ASSUMPTIONS

1. Space Shuttle

As previously mentioned, PANSAT will fly as a member of the Space Shuttle Small Self-Contained Payload (SSCP) program. An assumption as to when PANSAT would be ready for flight was made by using the tentative timeline indicated in Figure 15. This PANSAT schedule shows an expected launch in early 1997. By comparing Table 1 and Figure 15 an assumption that the very earliest PANSAT would fly would be on Space Shuttle Mission 80 (STS-80) with a proposed launch date of July 25, 1996. Therefore, an

analysis using PANSAT specific data and the proposed shuttle missions was performed from STS-80 through STS-99.

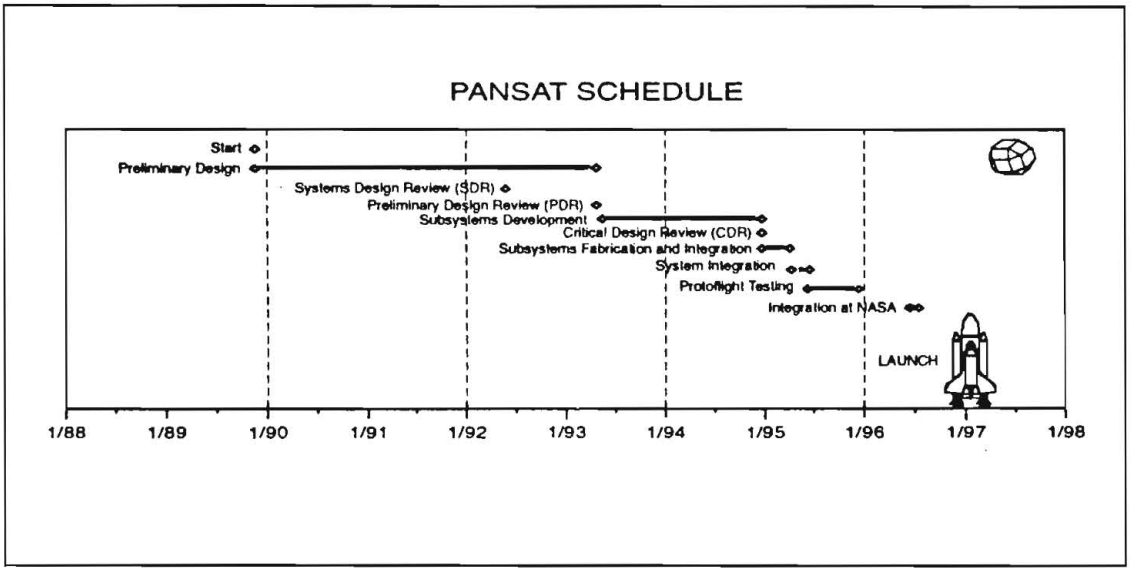

Figure 15. PANSAT Schedule

2. PANSAT Ballistic Coefficient

LIFETIME 4.1 provides the customer with the option of using an integration program to provide differential corrections to the ballistic coefficient input. The ballistic coefficient for PANSAT was calculated to be 36.2 lb/ft^2 or 176.4 kg/m^2 by equation (10) provided in Chapter II. The option of using differential corrections for the ballistic coefficient was not utilized due to the following:

1. the mass of PANSAT is not expected to change since no propulsion system is included and the mass is assumed evenly distributed throughout the spacecraft;
2. the area of PANSAT is constant because it very closely resembles a sphere and the solar panels are attached to the spacecraft body and are not appendages;

3. to use the differential coefficient option accurately, early observations of the semi-major axis, a, and eccentricity, e, are needed;
4. as per Wertz [Ref. 8:p. 207], the maximum and minimum ballistic coefficient for a sphere shaped satellite is the same: no change in Cd, mass or area results in no change in B.

3. F10.7 and Ap Data

F10.7 and Ap data was entered via three different ways. Analysis was done using the built in solar cycle, predicted values taken from Figure 16, and finally from a NASA document developed at the George C. Marshall Space Flight Center in Alabama [Ref.18].

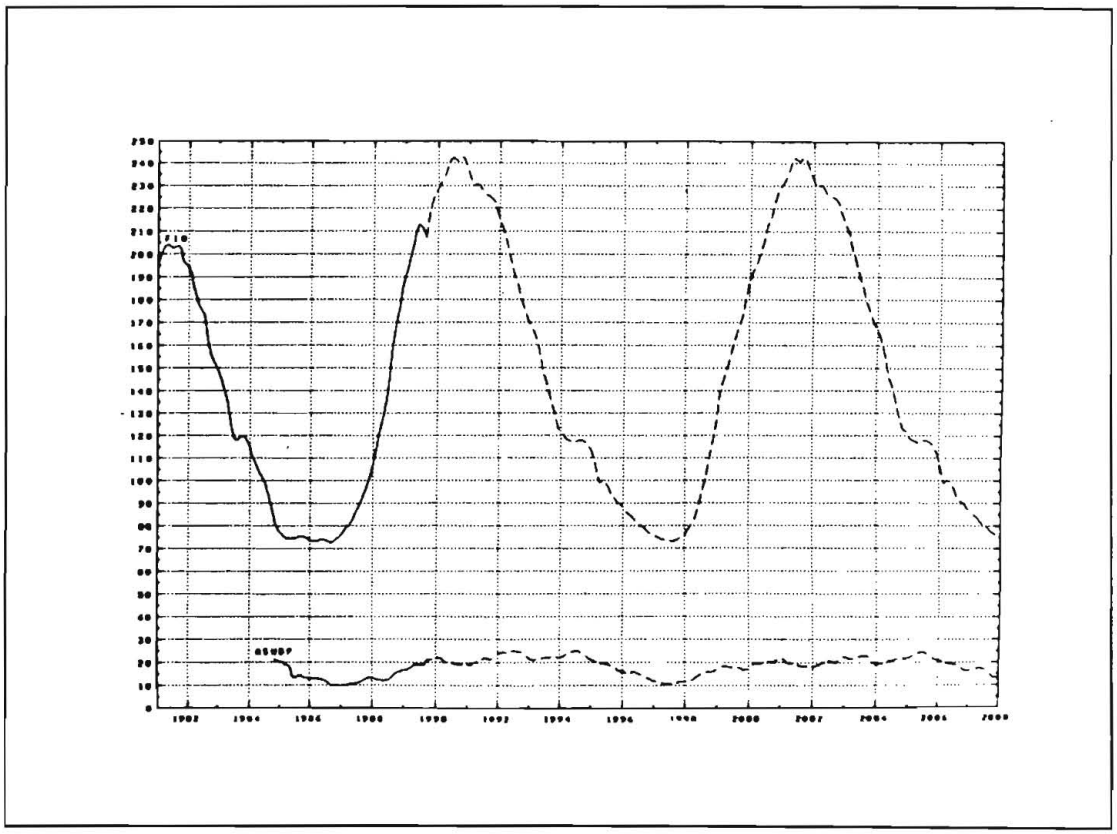

Figure 16. Observed and Predicted F10.7 and Ap Values [Ref. 12:p. 214]

The difference between default, predicted and NASA values of F10.7 and Ap are provided in Figures 17 through 20.

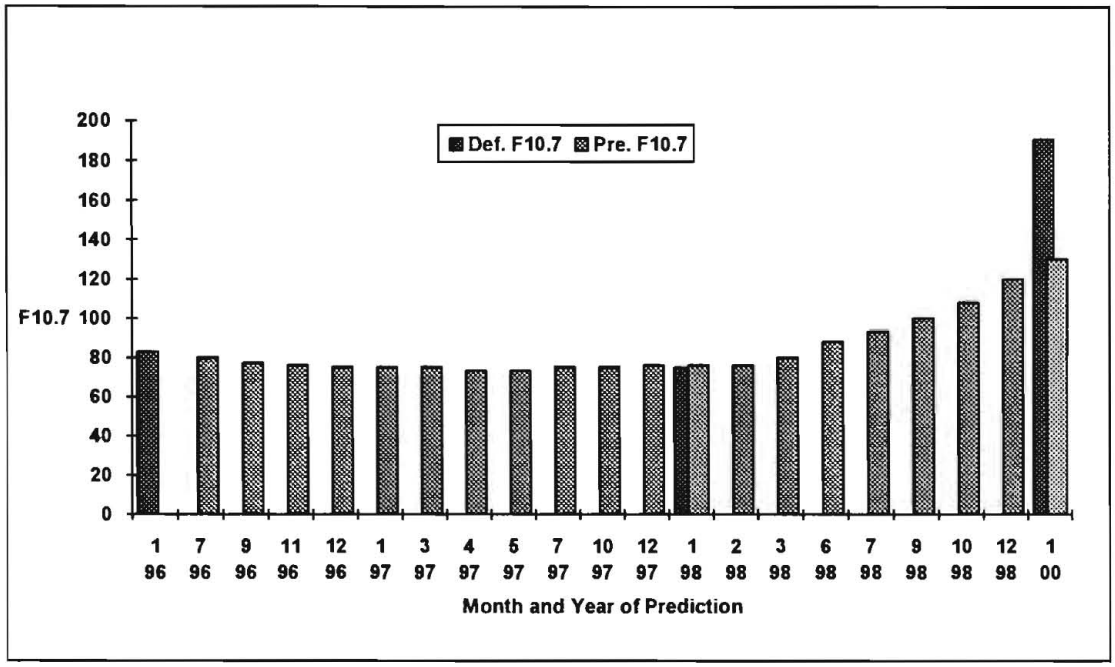

Figure 17. LIFETIME Unbiased Solar Cycle vs. Predicted Values (F10.7)

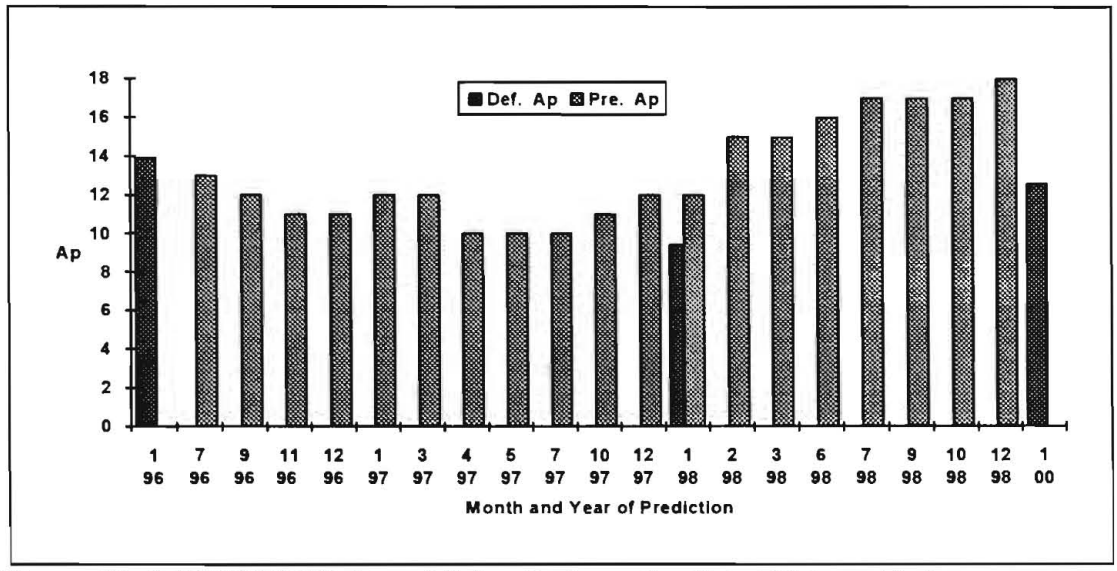

Figure 18. LIFETIME Unbiased Solar Cycle vs. Predicted Values (Ap)

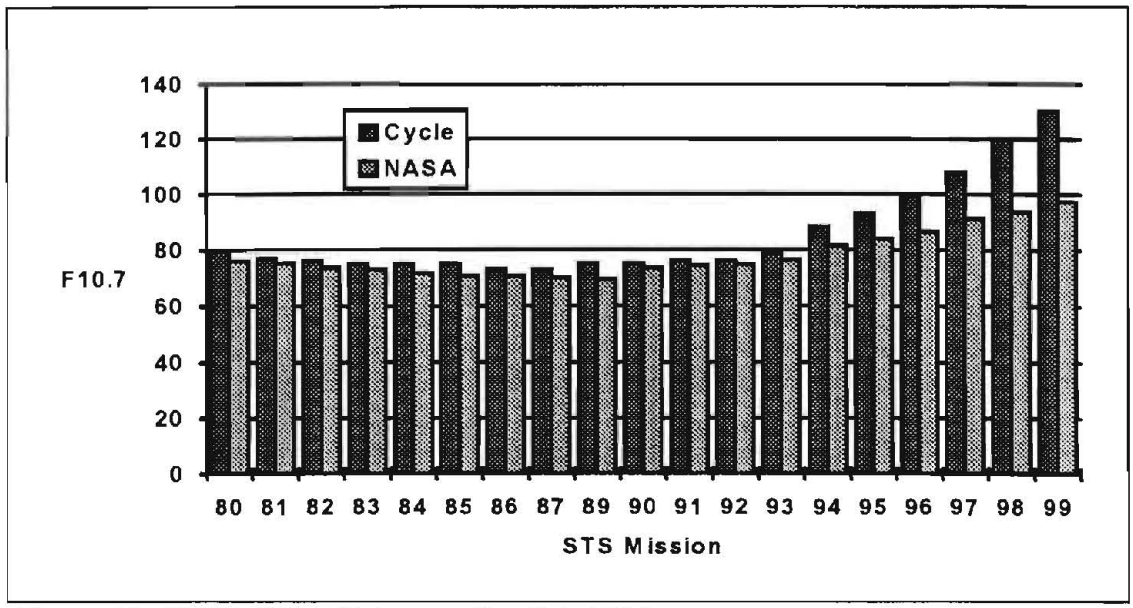

Figure 19. NASA F10.7 Values vs. Predicted Values

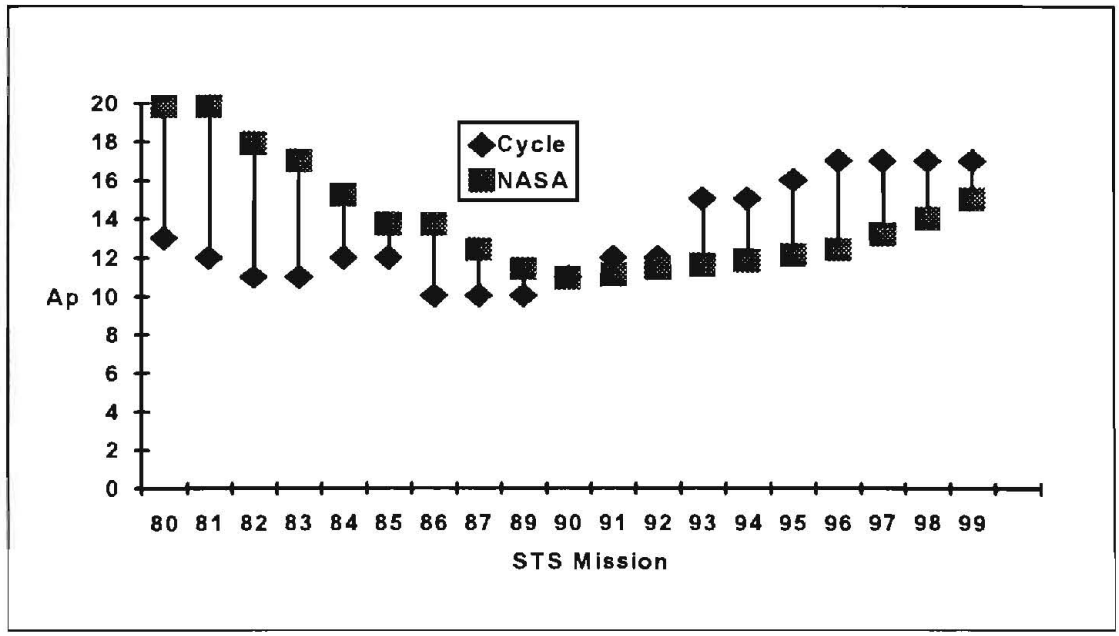

Figure 20. NASA Ap Values vs. Predicted Values

Figures 17 and 18 show that the default solar cycle supplies inputs only at two year intervals as illustrated by the darker columns. By comparison, the predicted and default values of F10.7 are closely related with the only difference being the rate of increase near the year of 2000 being higher for the default built in cycle . Conversely, Ap values differ with the predicted values rising faster than the default values. This difference does result in an increase in the number of shuttle missions that meet the two year orbital lifetime constraint.

Figures 19 and 20 also show a difference in the predicted values, which are labeled as 'cycle' on the graphs, and the projected NASA values which were estimated using a linear progression method of the previously observed solar cycle. The major difference noted in the two figures is that the NASA values rise at a slower rate than the values obtained from Figure 16. This change in projected increases is due to the linear rate of change being approximately 0.1503 for the F10.7 predicted data versus a linear rate of change of 0.0900 for the NASA data. Again, this difference results in the later expected shuttle missions meeting the two year constraint with the NASA data while STS missions 92 and beyond failing the two year requirement with the predicted values from Figure 16. These results are supplied in a following section.

4. Release Point in Orbit

LIFETIME allows the user to specify the release point in the orbit in order to predict the latitude and longitude of the impact point. Because the expected *launch* date, altitude, and time of release are unknown, the default values for the time was chosen as

01:00:00 and the default orbital elements were chosen as:

1. argument of perigee = 0.00^0;
2. longitude of ascending node = 0.00^0; and
3. true anomaly = 0.00^0.

5. Atmospheric Density Model

LIFETIME 4.1 provides the option of choosing either the Jacchia-Walker 1964 (analytical) or the Jacchia 1971 (numerical) atmospheric model. The model selected for PANSAT investigation was the Jacchia 1971 model. This is a dynamic model which uses the 1962 U.S. Standard Atmosphere below 90 km and incorporates both the solar flux (F10.7) and magnetic (Ap) indices. This model is widely used as the industry standard throughout the space community. The newest version of LIFETIME, LIFETIME 4.2, also includes the MSIS90E model as an option.

6. Propagation and Reentry Data

One of the last inputs needed for LIFETIME 4.1 is the time span for propagation along with the integration and breakup altitudes. LIFETIME integrates the equations of motion using a step size of multiples of the orbital period until the satellite reaches the specified or default altitude. An analysis done by Aerospace Corporation [Ref. 19], concluded that the breakup altitude for aluminum or magnesium spacecraft is 77.784 km or approximately 42 nmi. For the program to integrate the final phase of satellite reentry accurately, the program recommends an integration altitude above the breakup altitude,

so the default of 125 km was chosen. Also, the end of integration altitude was chosen as 0.00 km to model impact.

C. LIFETIME INPUTS

The following is list of the parameters used for initiating the LIFETIME program:

1. names of input, output and plotting files;
2. option of differential ballistic coefficient : not chosen due to reasons stated earlier;
3. epoch values :
   a) entered for the expected shuttle missions as per Table 1, starting with STS-80;
   b) January 30, 1997 selected as default date for extreme F10.7 and Ap and inclination analysis;
4. orbital elements selected as mean:
   a) a and i values entered as per Table 1;
   b) argument of perigee, longitude of ascending node and true anomaly values as per the assumption section;
5. ballistic coefficient entered as inverse of 36.2 lb/ft^2;
6. variation of ballistic coefficient caused by solar panels - not used;
7. atmospheric model - Jacchia 71;
8. F10.7 and Ap inputs:
   a) 11 year solar cycle
   b) predicted values with a linear rate of change depends on Figure 16
   c) NASA values
9. orbital sustenance not selected because of lack of propulsion system;
10. J_3 zonal harmonic not chosen due to the limited satellite lifetime expected
    a) it should be noted that several trial runs were conducted using J_3 with the change in expected lifetime ranging from only a few hours to less than a day;
11. time, step size, breakup/integration/end altitudes;

a) time - depending on shuttle altitude

b) step size - 1 orbital period [Ref. 15]

c) altitudes as per Table 1;

12. output options: plots.

D. LIFETIME RESULTS

1. Solar Flux and Magnetic Activity

Using the previously mentioned assumptions, an analysis of the effects of F10.7 and Ap values, along with changing the inclination of an orbit, was computed using LIFETIME 4.1. The analysis yield the expected results that the extreme values of F10.7 and Ap can dramatically influence PANSAT's lifetime. An unexpected result however, was the affect that a higher orbital inclination can have on the satellites lifetime. The inclination values used represent the lowest and highest shuttle inclinations advertised, 28.5^0 and 56.0^0 respectively [Ref. 2]. The latitude of Monterey, CA of $36^O35'$ was used since the controlling station will be housed at NPS, Monterey. An intermediate value of 45^O was also used for completeness. As Figure 21 illustrates, there can be a dramatic difference in the expected lifetime with a rise in the orbit inclination. For the lower extreme of F10.7 = 70.0 and Ap = 2, column A, the amount of increase in lifetime is on the order of 200 days. This increase is perhaps due to the fact that the satellite is periodically affected by the J_2 term in a higher inclined orbit, or in other words, spends less time in the orbital plane that is influenced by the J_2 harmonic.

The values charted below are:

Column A: F10.7 = 70 and Ap = 2;

Column B: F10.7 = 225 and Ap = 2;

Column C: F10.7 = 70 and Ap = 300;

Column D: F10.7 = 225 and Ap = 300.

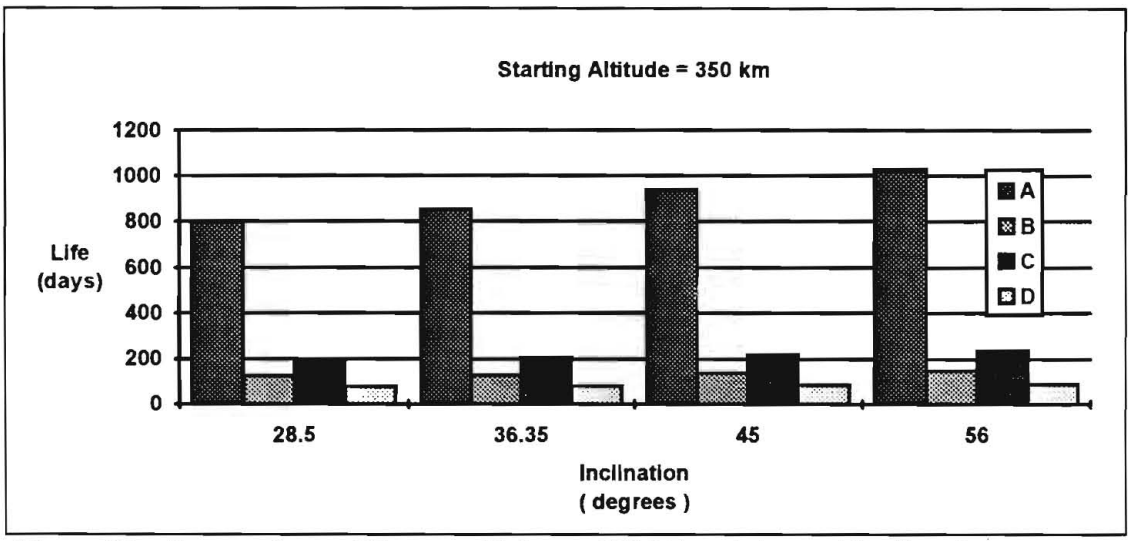

Figure 21. Comparison of Extreme Values of F10.7 and Ap and Inclination

2. Combining Data

Bringing together the Space Shuttle schedule, LIFETIME 4.1, the characteristics of PANSAT and the assumptions listed above allowed a prediction of anticipated PANSAT orbital lifetime using the shuttle as the insertion vehicle. Table 5 provides a breakdown of lifetime comparing the default values against the predicted values. It should be noted that a discrepancy was found on STS-85 regarding either the mission or the expected altitude. This disparity is that the predicted objective of the mission is to service the Hubble Space Telescope which is at 330 nmi or 611.2 km. Two separate *LIFETIME*

4.1 runs were made at the altitudes of 145 nmi (268.5 km) and 330 nmi (611.2 km) to cover both possibilities of objective or altitude error.

As can be seen from Table 5, the difference in lifetimes, "Delta Lifetime", was relatively close except for STS missions 85B and 88. The reason for the discrepancy is that at the projected insertion altitudes the expected lifetime covers an entire solar cycle. Therefore, the predicted values entered were the average values over a solar cycle with F10.7 = 150 and Ap = 12. Other disagreements occur because of the difference in input values along with manually entering F10.7 and Ap values near the trough and peak of the solar cycle curve cannot be correctly adjusted using just the linear rate of change option. Near these peaks and valleys, it is suggested to enter the F10.7 and Ap values by the "vector" option in LIFETIME. The "vector" method, however, was not an option using Figure 16 for predicted values.

By using a conservative approach, only the STS missions that provided a minimum of two years of lifetime for PANSAT were singled out as acceptable missions. Most of these missions occur in late 1996 and early 1997 and coincide with the solar minimum. Table 6 provides a listing of the missions that meet the requirements for expected lifetime. The listing provided in Table 6 was entered into a spreadsheet utilizing the equations provided at the end of reference [8] to explore a few of the orbital characteristics of PANSAT if inserted on the acceptable STS missions. The parameters explored and provided in Table 7 included period, maximum eclipse time, and maximum time in view for a satellite in circular orbit passing directly over a ground station. It should be noted

that if PANSAT is inserted at an inclination of only 28.5^{O}, the true maximum time in view at NPS will be less than the value in Table 7.

TABLE 5. PROJECTED PANSAT LIFETIME

Flight	Altitude (km)	Default LIFETIME	Predicted F10.7	Predicted Ap	Predicted LIFETIME	Delta LIFETIME
STS - 80	394.5	1190	80	13	1371	181
STS - 81	394.5	1360	77	12	1488	128
STS - 82	296.3	112	76	11	115	3
STS - 83	394.5	1564	75	11	1593	29
STS - 84	394.5	1589	75	12	1551	38
STS - 85A	268.5	47	75	12	47	0
STS - 85B	611.2	10078	150	12	14640	4562
STS - 86	351.9	486	73	10	486	0
STS - 87	394.5	1046	73	10	927	119
STS - 88	574.1	6130	150	12	8459	2329
STS - 89	407.4	1058	75	10	832	226
STS - 90	394.5	632	75	11	624	8
STS - 91	407.4	732	76	12	726	6
STS - 92	394.5	682	76	12	682	0
STS - 93	407.4	721	80	15	683	38
STS - 94	394.5	648	88	15	610	38
STS - 95	407.4	645	93	16	620	25
STS - 96	407.4	614	100	17	582	32
STS - 97	407.4	575	108	17	544	31
STS - 98	407.4	544	120	17	502	42
STS - 99	407.4	502	130	18	468	34

TABLE 6. ACCEPTABLE SPACE SHUTTLE MISSIONS

Flight	Launch Date	Inclination	Altitude (km)	Conservative LIFETIME (days)
STS - 80	7/25/96	51.6	394.5	1190
STS - 81	9/6/96	51.6	394.5	1360
STS - 83	12/5/96	51.6	394.5	1564
STS - 84	1/30/97	51.6	394.5	1551
STS - 85B	3/27/97	28.5	611.2	10078
STS - 87	5/30/97	51.6	394.5	927
STS - 88	6/26/97	28.5	574.1	6130
STS - 89	7/31/97	28.5	407.4	832
STS - 91	12/4/97	28.5	407.4	730

The actual time in view for PANSAT at various altitudes and elevation angles are provided by Sakoda [Ref. 20], with a 10^{O} elevation angle providing between 5 to 7 minutes at a 28.5^{O} inclination. The maximum eclipse time calculated in Table 7 coincides with a previous analysis and the finding of roughly 39 % of the orbital period possibly in eclipse.

To summarize, PANSAT lifetime dramatically depends on F10.7 and Ap values in conjunction with the altitude of orbit insertion. This is easily seen in Figure 22, which projects PANSAT's life span as a function of the solar cycle and starting altitude. This figure was interpolated from Wertz and Larson [Ref. 8: p.211] using the ballistic coefficient calculated for PANSAT.

TABLE 7. PANSAT ORBITAL PARAMETERS / SPACE SHUTTLE INSERTION

STS Mission	80-84&87	85B	88	89 & 91
Inclination (deg)	51.6	28.5	28.5	28.5
h (km)	394.5	611.2	574.1	407.4
u (km^3/s^2)	398601.2	398601.2	398601.2	398601.2
Re (km)	6378.15	6378.15	6378.15	6378.15
inclination (rad)	0.90059	0.497419	0.497419	0.497419
Area (m^2)	0.175	0.175	0.175	0.175
Mass (kg)	68.04	68.04	68.04	68.04
Cd	2.2	2.2	2.2	2.2
r (km)	6772.65	6989.35	6952.25	6785.55
rhomin (kg/m^3)	2.62E-12	9.89E-14	1.59E-13	2.52E-12
rhomax (kg/m^3)	1.05E-11	8.46E-13	1.2E-12	1E-11
circular velocity (km/sec)	7.671671	7.551807	7.57193	7.664375
period (min)	92.44803	96.92034	96.14967	92.71229
angular velocity (deg/min)	3.89408	3.714391	3.744163	3.88298
Earth Angular Radius (deg)	70.34773	65.86053	66.55212	70.04495
0 elev (deg)	19.65227	24.13947	23.44788	19.95505
5 elev (deg)	15.25394	19.62143	18.94556	15.5471
10 elev (deg)	11.9602	16.01371	15.38001	12.22877
Max Time in View @ 0 (min)	10.09341	12.99781	12.52503	10.27821
Max Time in View @ 5 (min)	7.834426	10.56509	10.12005	8.007817
Max Time in View @ 10 (min)	6.142759	8.622522	8.215459	6.298654
Orbit Decay Rate (km/yr)	-24.341	-0.93341	-1.49664	-23.4343
Max Orbit Decay Rate (km/yr)	-97.55	-7.98449	-11.2954	-92.9932
Rev/day	15.53381	14.81701	14.93578	15.48953
Max eclipse (min)	36.13061	35.46236	35.5498	36.07793
Node Spacing (deg)	23.17526	24.29639	24.1032	23.2415
Node precession Rate (deg/day)	-5.01655	-6.35675	-6.47627	-7.05044

By comparison, Table 8 shows the necessary starting altitudes for 2, 3 and 4 year lifetimes dependent on different values of F10.7 and Ap for PANSAT. These same results are portrayed in Figure 23 developed with the expected solar flux and magnetic values for a launch in late 1996 or early 1997.

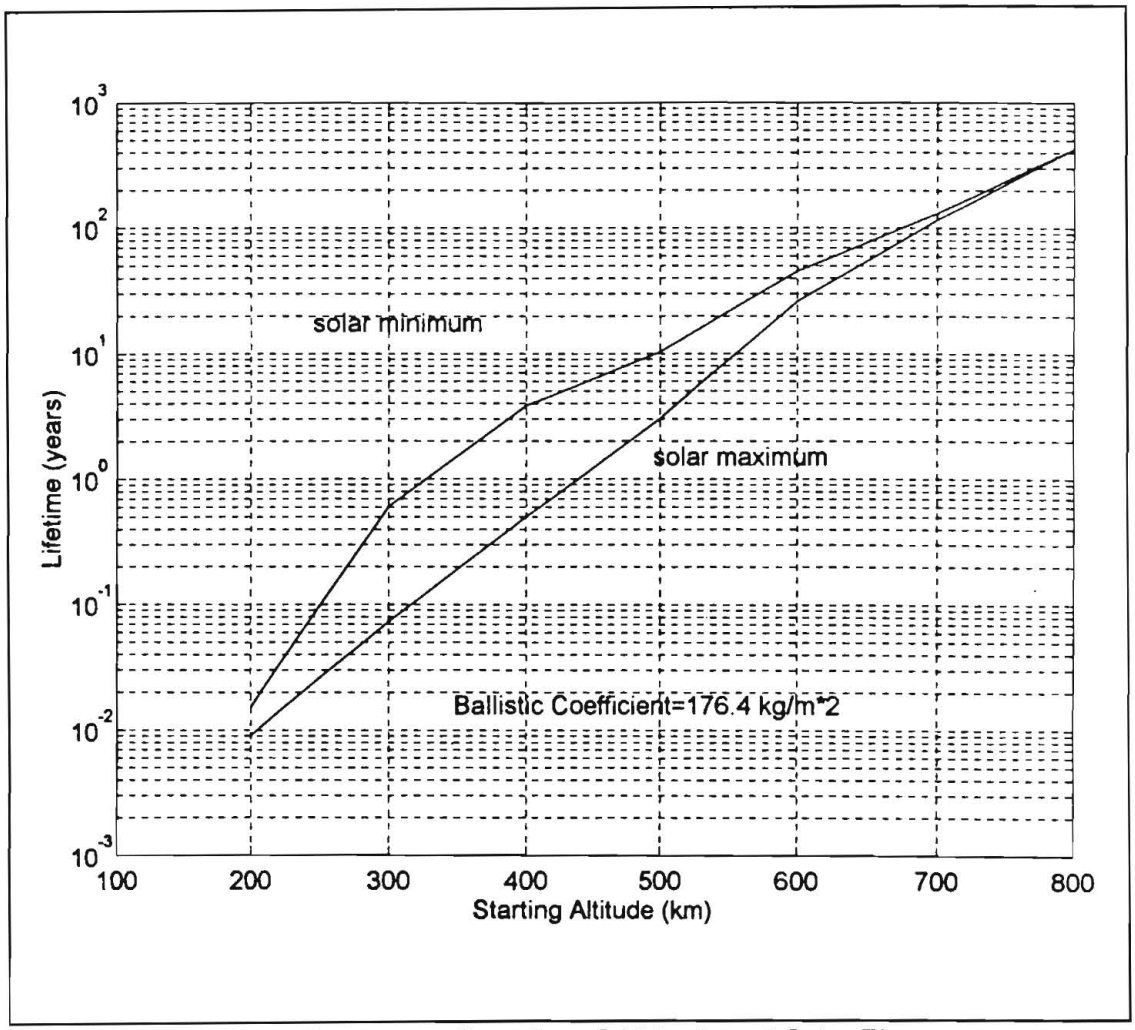

Figure 22. Satellite Lifetime as a Function of Altitude and Solar Flux

TABLE 8. REQUIRED STARTING ALTITUDES FOR VARIOUS F10.7/AP

LIFETIME	F10.7 = 73 Ap = 10	F10.7 = 100 Ap = 15	F10.7 = 150 Ap = 20
2 years	370 km	390 km	430 km
3 years	385 km	410 km	450 km
4 years	400 km	425 km	470 km

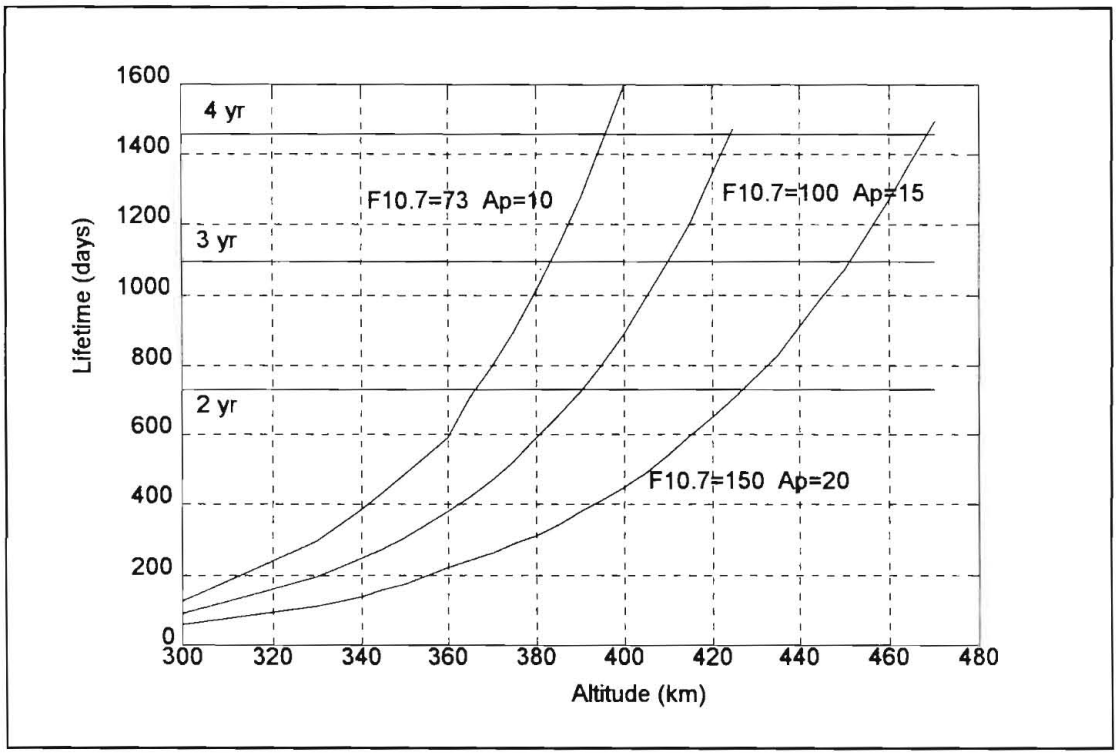

Figure 23. Orbit Lifetime vs. Starting Altitudes and F10.7 / Ap Values

V. PANSAT REENTRY

A. INTRODUCTION

The Petite Amateur Navy Satellite (PANSAT), like all other low-earth-orbiting satellites, will eventually end its journey by reentering into the Earth's atmosphere. This leads to the final phase of PANSAT's lifespan known as the "reentry phase".

There are various types of spacecraft reentry trajectories that can be classified into two groups: controlled and uncontrolled. A controlled reentry is typical of a trajectory where the vehicle's aerodynamic and heating loads are limited or maintained resulting in the vehicle surviving reentry to impact or land at a specified point. The basic requirement for surviving is manipulation of the lift and drag forces in order to control the flight path angle and thus the loads imparted on the vehicle. Typical types of controlled reentries are:

1. ballistic - characterized by steep reentry angles typical of missiles,
2. gliding - the lift created by the reentering vehicle, such as the Space Shuttle, allows a long hypersonic glide at a reduced flight path angle,
3. skip - the vehicle's lift can offset the gravitational forces causing a change in the flight path angle permitting the vehicle to obtain orbit at a reduced velocity.

An uncontrolled trajectory is typical of an unrecoverable satellite reaching its end of operational life. For such a reentry, the vehicle's lift capability is negligible and the flight path angle is generally much less than 1^0. Figure 24 illustrates the different types of reentries [Ref. 14: p.18-20]. The purpose of this section is to explain the environment and predict the survivability of PANSAT in the reentry phase.

B. PANSAT'S ORBITAL DECAY

1. Reentry

There exists many different theories, formulations, and analytical, semi-analytical and numerical solutions to predict reentry of satellites. Scrutiny of equations of motion, rarefied gas dynamics, material specifics, various heating and load effects and satellite characteristics are among the many topics that must be considered in the prediction of satellite reentry and survivability. Henderson and Neuenfeldt [Ref. 14] provide an excellent literature search and summary of many methods employed today for reentry analysis. It is not the purpose of this thesis to delve into all of the subjects in order to predict PANSAT's survivability as each of these topics provides an in-depth thesis opportunity for others. The direction taken, therefore, is a brief synopsis of the expected happenings that will influence PANSAT's reentry ending with a prediction of survivability. Since PANSAT will have no attitude control nor propulsion systems and the physical characteristics will allow virtually zero lift, it will follow the trajectory of a decaying orbit classifying it as a uncontrolled entry. The major conditions influencing an uncontrolled reentry and survivability are a rapid decrease in altitude, an abrupt increase in aerodynamic heating loads and a significant increase in aerodynamic loads.

In addition to being classified as uncontrolled, PANSAT's reentry can also be divided between the flight before and after satellite breakup, the point in the trajectory where aerodynamic heating and load effects cause a failure in the structural integrity of the spacecraft.

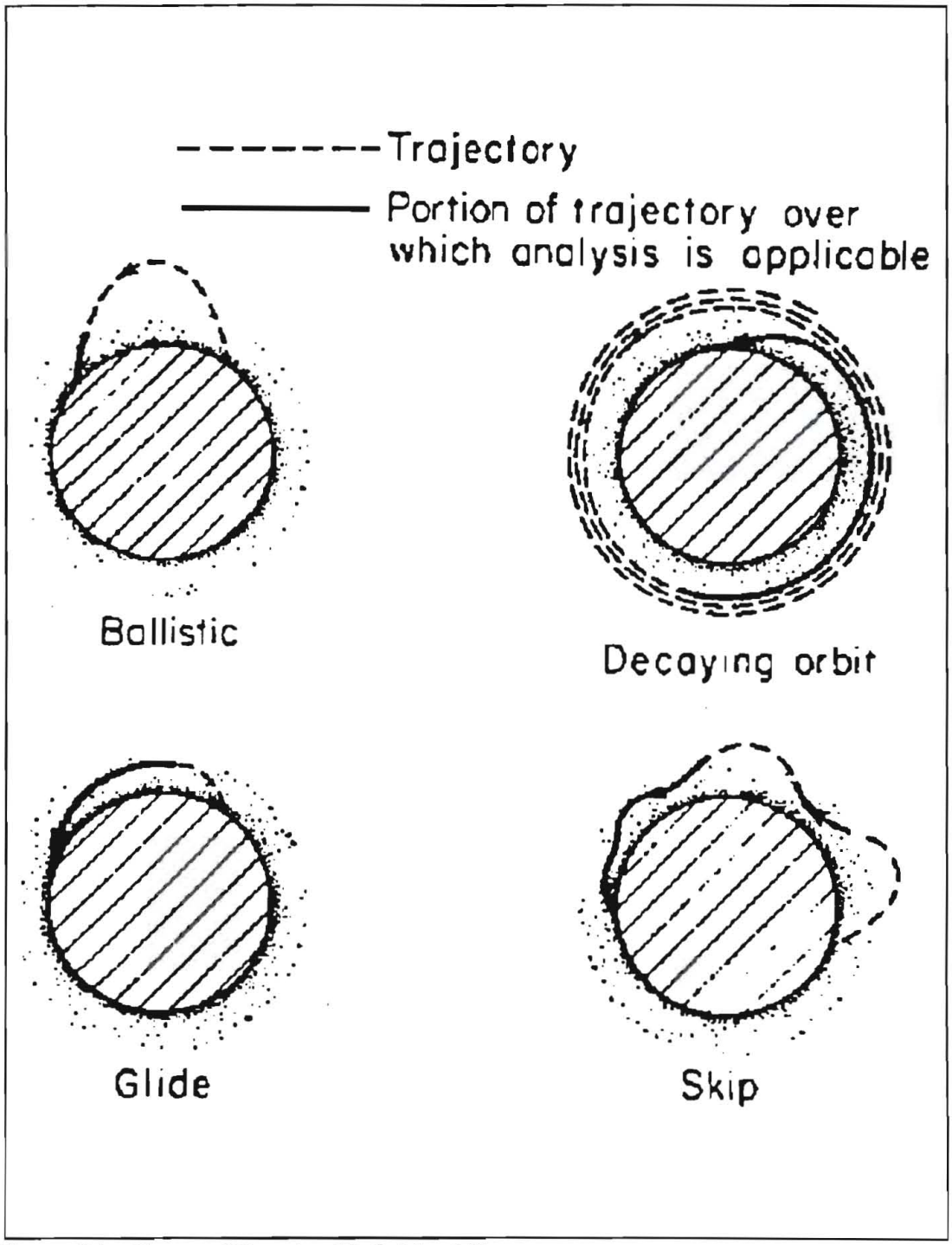

Figure 24. Types of Reentry [Ref. 14:p.19]

2. Aerodynamic Heating

The basics behind the heating of a reentering satellite include the exchanging of kinetic energy into heat. During this phase, the velocity of the satellite is continually converted into heat through atmospheric drag. The energy balance is

$$\frac{Q}{W} = \frac{V^2}{2g} \tag{28}$$

where Q is the dissipated heat, W is the satellite weight, and g the gravitational constant. For a velocity, V, equal to a orbital speed of 26,000 ft/sec (7.925 km/sec), Q/W = 13,500 Btu/lb which is sufficient to vaporize most any spacecraft material except for possibly graphite. However, this isn't necessarily the case for aerodynamic heating. [Ref. 14:p. 5] Two major processes, the formation of a shock wave and radiation heating, divert energy away from the spacecraft and thus reduce the amount of heating.

At a very high altitude, known as free-molecular flow region, up to one half of the kinetic energy may be converted into heat [Ref. 14:p. 44]. However, since the flight path angle is extremely shallow and atmospheric density is low, there is very little deceleration and conversion of energy. In the continuum flow regions typified in lower altitudes, a shock wave develops ahead of the vehicle which creates a boundary layer through which heat must pass. This transfer of heat occurs in the forms of conduction and convection and in conjunction with radiation heating from hot gases, contributes to the total amount of heat the vehicle experiences.

Three aspects of aerodynamic heating were found to be significant [Ref. 14:p.45]:

1. the total heat input;

2. the time rate and maximum time rate of local stagnation region heat input per unit area;
3. the time rate and maximum time rate of average heat input per unit area.

Figure 25 [Ref. 21:p. 4] depicts the shock wave and stagnation temperature on a reentry vehicle with Table 9 [Ref. 21:p. 5] providing stagnation temperatures expected for a vehicle reentering Earth at several velocity values adjustable by lift to drag ratios.

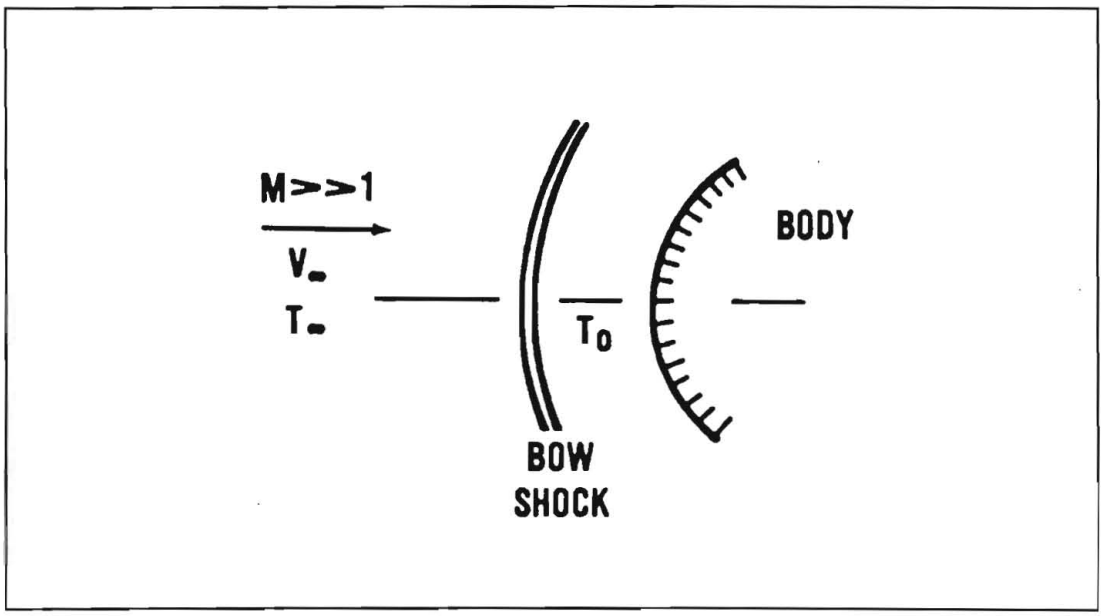

Figure 25. Shock wave and Stagnation Temperature on a Reentering Vehicle

TABLE 9. STAGNATION TEMPERATURES

Velocity (ft/sec)	T_o, ^oR
10,000	8,325
20,000	33,300
26,000	56,277

Aerospace Corporation has conducted a review of heating rates versus altitude for aluminum and magnesium structures as a function of ballistic coefficients. Figure 26 provides the results of the study in the form of a graph. The vertical column in the figure represents the melting point for aluminum and magnesium structures. By inspection of the graph it is shown that such structures with ballistic coefficients greater than or equal to approximately 15 lb/ft^2 will reach a heating rate that should be sufficient for material melting. Since PANSAT has a ballistic coefficient of 36.2 lb/ft^2, it is safe to assume that the outer structure will melt upon reentry.

3. Aerodynamic Loading

The amount of aerodynamic loads that PANSAT will experience depends on the rate of deceleration of the satellite. In turn, deceleration is a product of air density and velocity. As PANSAT descends further into Earth's atmosphere, the density will dramatically increase resulting in atmospheric drag forces slowing the satellite's velocity. However, at some altitude the velocity decrease occurs faster than the density increase. It is at this point in reentry that PANSAT will experience its maximum deceleration resulting in a peak of aerodynamic loading. This dependence on density and velocity is illustrated in Figure 27 for both the deceleration and heating rates for a satellite.

In an analysis presented by Hankey [Ref. 21:p.33-36], an orbital decay always produces a 8g deceleration which is independent of the ballistic coefficient. This result closely matches with the Aerospace Corporation study [Ref. 19] of load factor versus

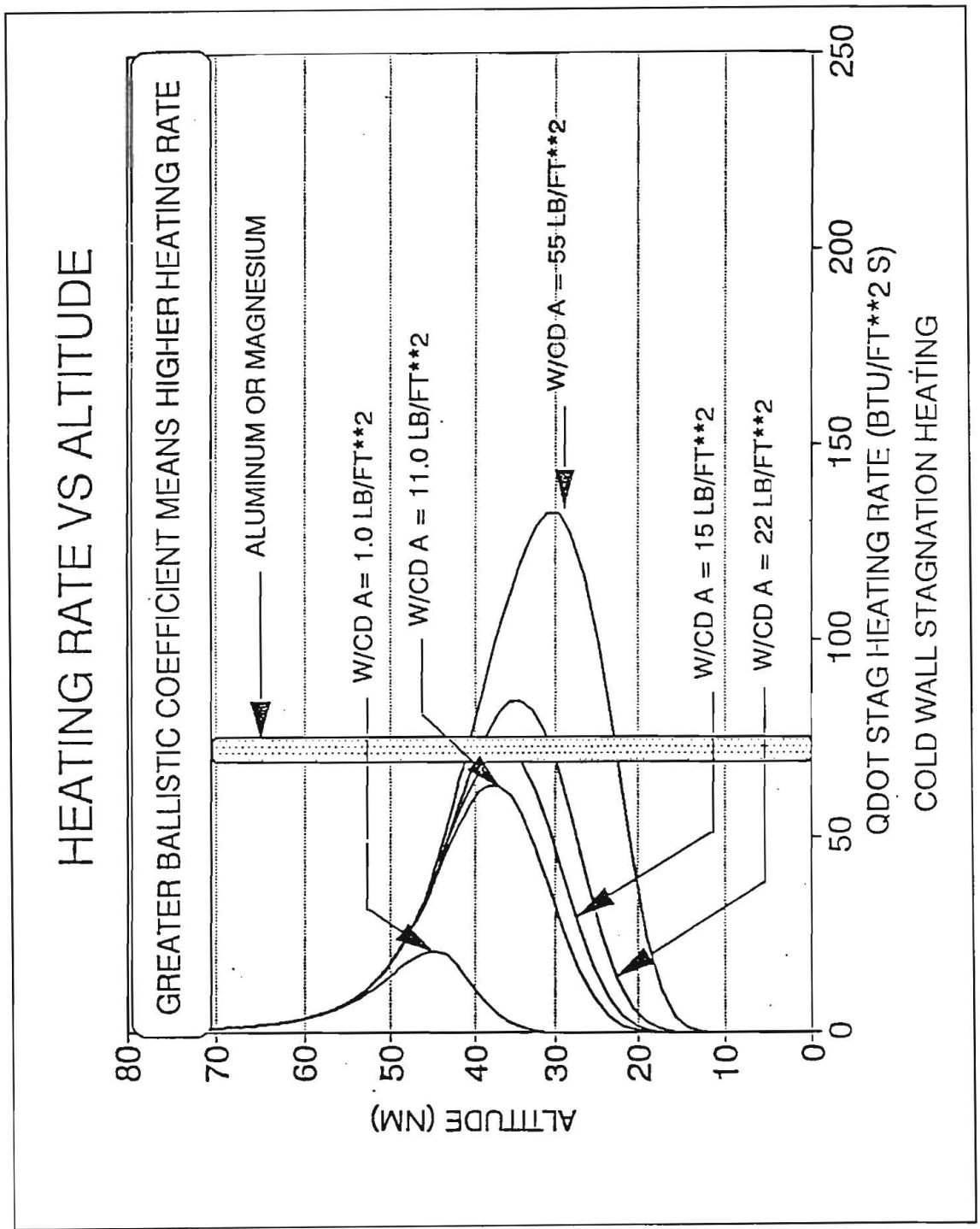

Figure 26. Heating Rate vs. Altitude for Varied Ballistic Coefficients [Ref. 19]

altitude for various ballistic coefficients as shown in Figure 28. By comparing Figures 26, 27 and 28, it is also shown that maximum loading occurs at a lower altitude than maximum heating. This may prove to be beneficial since PANSAT will most likely experience melting prior to an 8g loading and thus will expose the internal components to the atmosphere for destruction.

4. Structural Failure and Breakup

The previous sections explained the dynamic processes and their effects that PANSAT is expected to encounter on reentry. It is hoped that reentry will result in a breakdown in structural integrity of PANSAT with complete destruction of all its components.

The dominant factor influencing structural failure is the ability of the vehicle to exceed its melting temperature, which in turn, is a function of heating rate and ballistic coefficient. A higher ballistic coefficient results in higher heating rates and thus higher equilibrium temperatures that the vehicle will encounter [Ref. 19:p.18]. Findings taken from an Aerospace Corporation publication [Ref. 19], are summarized as:

1. consistent catastrophic failure of aluminum structures is at an altitude of 42 nmi or 77.78 km for ballistic coefficients of 15 lb/ft^2 or greater;
2. breakup phenomena is independent of vehicle attitude, diameter and shape and entry path angles of less than 1.5^0.

The Aerospace Corporation study [Ref. 19] used extensively in PANSAT's reentry analysis was also included in the LIFETIME 4.1 input for the 42 nmi breakup altitude to predict the impact footprint.

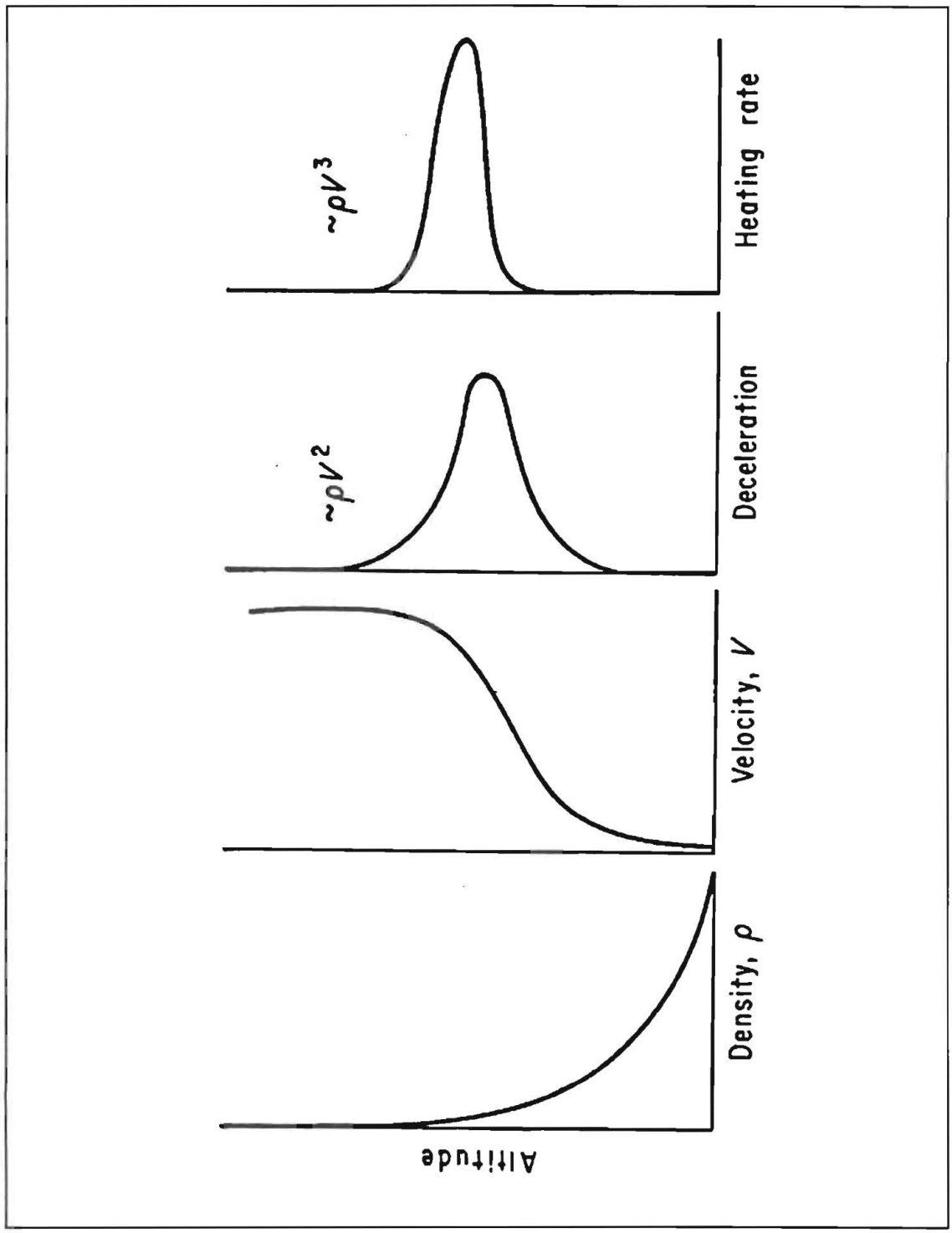

Figure 27. Deceleration and Heating Dependence on Density and Velocity [Ref. 14]

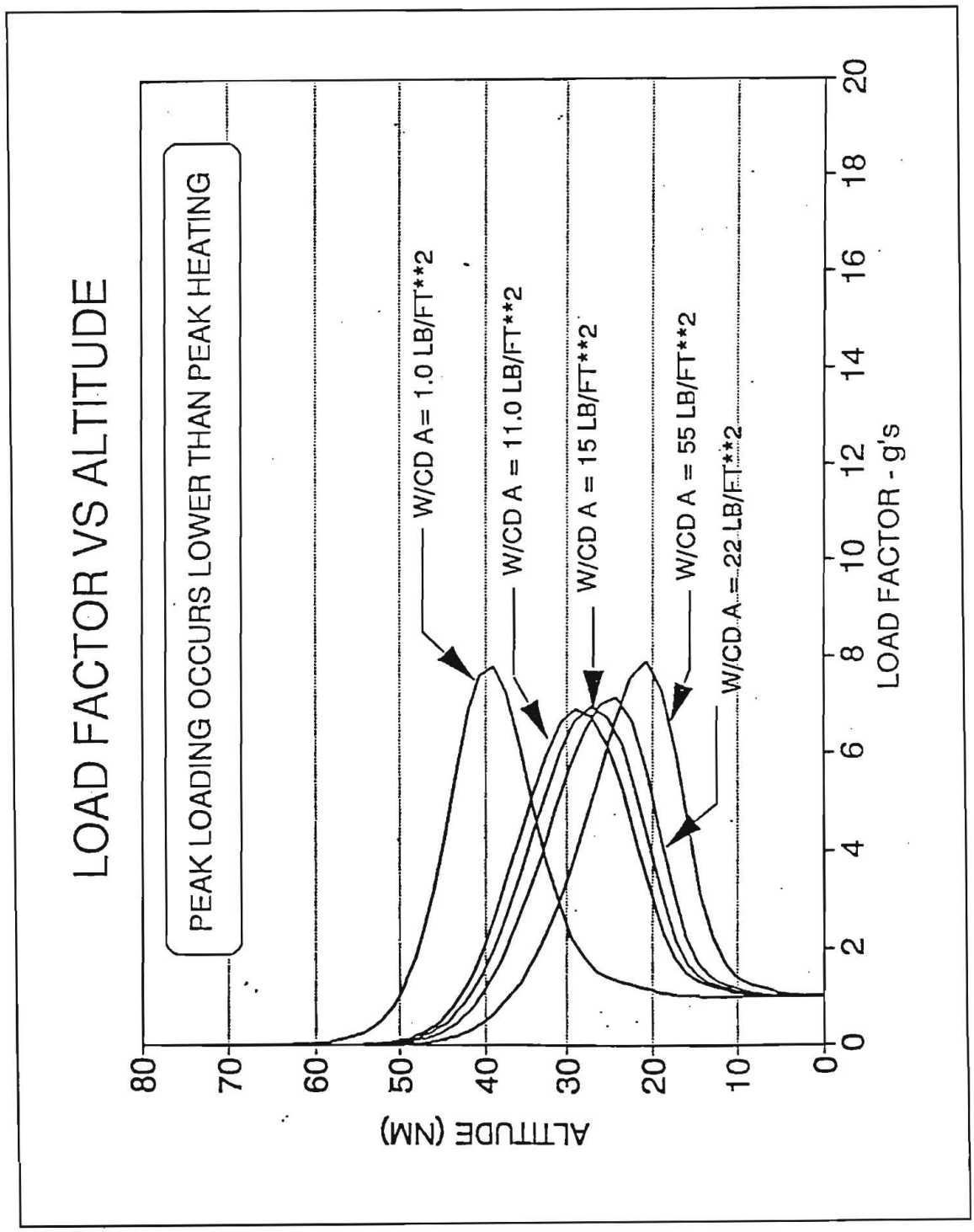

Figure 28. Load Factor vs. Altitude for Various Ballistic Coefficients [Ref. 19]

5. Survivability to Impact

PANSAT does not have a deboost capability which would allow disposal in broad ocean areas. As concluded in section 4 above, PANSAT is expected to encounter sufficient aerodynamic heating and structural loads to predict a failure of the outer casing. However, the possibility of debris surviving to impact must be considered as the internal materials are exposed to the atmosphere. Aerospace Corporation proposed the following criteria for survival: [Ref. 19: p.C9]

1. ballistic coefficient and material of objects dictates survivability;
2. objects with low ballistic coefficients typically survive;
3. objects with higher melting temperatures can survive with higher ballistic coefficients;
4. survivability of objects is much greater than has been and continues to be analytically predicted.

Therefore, after breakup, PANSAT subcomponents may have ballistic coefficients low enough to allow a rapid deceleration through their peak heating resulting in survivability to impact. It has been shown that objects with ballistic coefficients lower than approximately 15 lb/ft^2 for aluminum structures typically survive reentry. Another factor in survivability is the internal material's melting temperature. In fact, circuit boards have survived reentry showing little evidence of heating and have only been identified as reentry debris by association with a suspected satellite impact area [Ref. 19]. Table 10 provides the melting temperatures for the expected materials used in PANSAT construction.

TABLE 10. MATERIAL MELTING TEMPERATURES

Material	Melting Temperature, ^{o}F
Aluminum	1220
Cadmium	610
Nickel	2651
Ceramic	3092 (fusing temperature)
Silicon	2588

Prediction of potential impact areas thus acquire importance due to the possibility of casualties and property damage. There have been many attempts to analyze the hazard of reentry such as random reentry risk evaluation programs by LMSC and TRW . A review of risk predictions was included in Aerospace Corporation study [Ref. 19]. This review is used by the LIFETIME 4.1 program in its analysis. LIFETIME 4.1 provides an expected latitude and longitude of impact footprint as shown in Figure 13 of Chapter III. When the release point of PANSAT has been verified, utilizing the LIFETIME program may provide enough time for notification of the casualty area.

VI. CONCLUSIONS AND RECOMMENDATIONS

The artistry of satellite lifetime prediction depends on the ability to estimate many variables in combination with scientific findings. Even the "state-of-the-art" methods, which are based on years of study and analysis, still find themselves fundamentally inadequate to account for all of the variations of satellite environment that affect lifetime. An example is that F10.7 and Ap values, which have been monitored for years, still present a immense challenge in terms of prediction. Studies of atmospheric density modeling, estimation of the coefficient of drag, and their effects on atmospheric drag have produced notable advances in the area of orbital lifetime. However, the assumptions used in the examination of these topics are of themselves open for debate in terms of their validity.

LIFETIME 4.1 has been found to be a simplified yet rather accurate tool in the continuing effort of understanding and estimating a satellite's orbital life. The results provided by this thesis are biased on the conservative side regarding the altitude and launch dates in order to provide PANSAT users a minimum of two years of operational life. Taking into account the many assumptions made throughout the analysis, Table 6 in Chapter IV suggests that a late 1996 through 1997 launch will supply the 2 year life span required of PANSAT. To simplify the analysis further, if PANSAT is released into an orbit of approximately 410 km with F10.7 and Ap values of no higher than 94 and 14 respectively, and with a linear rate of change of F10.7 of no greater than 0.09 per day, it will meet the 2 year lifetime constraint.

Other conclusions formed as a result of this thesis is that the J_3 harmonic effect will have little influence on PANSAT's life whereas change to a higher inclination can add up to approximately 200 days of operational life. The higher inclination also provides an advantage in terms of time in view of PANSAT to the ground station housed at NPS but will add a small disadvantage for PANSAT in the reentry phase because as a satellite's orbital inclination increases, the probability of surviving debris impacting land also increases. This is simply due to the fact the amount of time a satellite spends over land increases with the inclination of the satellite. The probability of land impact versus inclination angle is depicted in Figure 29.

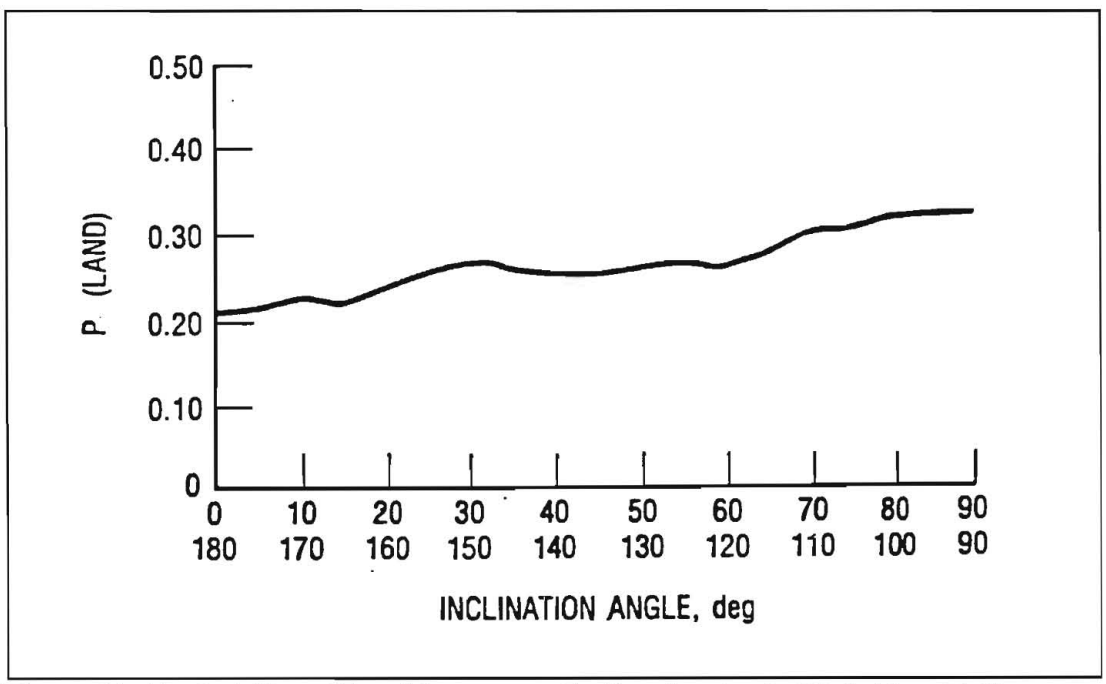

Figure 29. Probability of Land Impact vs. Inclination Angle [Ref. 19:p. B-3]

The reentry phase of PANSAT presents an entirely different issue than the lifetime prediction. One similarity, though, is that the uncertainties of atmospheric density and

drag models induce errors in predicting survivability as well as lifetime. Best estimates imply that at least the outer structure of PANSAT will be destroyed on reentry. However, the endurance of the internal components is still in question.

Recommendations proposed by this study are as follows:

1. to help ensure complete destruction of PANSAT and all of it's components, the ballistic coefficients of all internal parts such as the batteries should be as high as possible to help in the heating effect
2. materials of lower melting temperatures should be used whenever feasible
3. the earlier PANSAT can be inserted into orbit, the lower the required altitude to maintain reasonable assurances of meeting a 2 year life, therefore a late 1996 or early 1997 launch is urged
4. a new or updated link analysis should be done to ensure operational satellite to ground communications at the Space Shuttle altitude limit of 612 km since PANSAT's power generation subsystem may not provide the necessary energy required for that altitude
5. after insertion with the opportunity to observe the exact epoch values, orbital elements and insertion point, as well as the observed semi-major axis and eccentricities for differential ballistic coefficient corrections, the LIFETIME program should be run to provide updated lifetime and reentry/impact estimations.

In closing, this research opened up a variety of future thesis opportunities such as a comparison of LIFETIME 4.1 predictions to those of other orbital lifetime propagators , a complete reentry heating analysis using the most advanced methods and investigations of other possible launch vehicles if a shuttle launch is ruled unlikely.

LIST OF REFERENCES

[1] Sakoda, D. J., *Structural Design, Analysis, and Modal Testing of the Petite Amateur Navy Satellite (PANSAT)*, Master's Thesis, Naval Postgraduate School, Monterey, CA, September 1992.

[2] Johnson Space Center, NASA FAX, Subject: *Space Shuttle Altitudes and Inclinations*, April 1994.

[3] Agrawal, B. N., *Design of Geosynchronous Spacecraft*, Prentice-Hall, Inc., Englewood Cliffs, NJ, 1986.

[4] Harwood, W., *NASA Long-Term Plan For Shuttle Missions Details Station Timing*, Space News, Vol. 5, No. 10, March 1994.

[5] National Aeronautics and Space Administration, *Space Station Freedom User's Guide*, NASA, Washington DC, August 1986.

[6] Chao, C. C., and Platt, M. H., *An Accurate and Efficient Tool for Orbit Lifetime Predictions*, AAS Paper 91-134, AAS/AIAA Spaceflight Mechanics Meeting, Houston, Tx, 1993.

[7] Szebehely, V. G., *Adventures in Celestial Mechanics*, University of Texas Press, Austin TX, 1989.

[8] Larson, W. J., and Wertz, J. R., *Space Mission Analysis and Design*, Microcosm, Inc., Torrance, CA, 1992.

[9] Roy, A. E., *Orbital Motion*, Adam Hilger Ltd, Bristol, UK, 1982.

[10] Tascione, T. F., *Introduction To The Space Environment*, Orbit Book Company, Inc., 1988.

[11] Adler, J. J., *Thermospheric Modeling Accuracies Using F10.7 & Ap*, Master's Thesis, Naval Postgraduate School, Monterey, CA, December 1993.

[12] Chobotov, V. A., *Orbital Mechanics*, AIAA, Inc., Washington DC, 1991.

[13] Bowden, B., *The Use Of Atmospheric Models in Orbit Prediction*, paper presented at Naval Postgraduate School, Monterey, CA, December 1993.

[14] Neuenfeldt, B. D., and Henderson, W. K., *A Survey of Uncontrolled Satellite Reentry and Impact Prediction*, Master's Thesis, Naval Postgraduate School, Monterey, CA, September 1993.

[15] Chao, C.C., and others, *Re-entry Impact Point Prediction Using NORAD Elements*, AAS Paper 94-159, AAS/AIAA Spaceflight Mechanics Meeting, Cocoa Beach, FL, 1994.

[16] Liu, J. J. F., and Alford R. L., *Semianalytic Theory for a Close-Earth Artificial Satellite*, Journal of Guidance and Control, Vol. 3, No. 4, July-August 1980.

[17] Strizzi, J. D., *An Improved Algorithm For Satellite Orbit Decay And Re-Entry Prediction*, Master's Thesis, Massachusetts Institute of Technology, June 1993.

[18] Causey, W. E., *Solar Activity Inputs for Upper Atmospheric Models Used in Programs to Estimate Spacecraft Orbital Lifetimes*, National Aeronautics and Space Administration, Marshall Space Flight Center, May 1992.

[19] Refling, O., Stern, R.. and Potz, C., *Review of Orbital Reentry Risk Predictions*, ATR-92(2835)-1, The Aerospace Corporation, El Segundo, CA, July 1992.

[20] Sakoda, D. J., *PANSAT Orbit Analysis and Ground Station View*, paper presented at Naval Postgraduate School, Monterey, CA, 1993.

[21] Hankey, W. L., *Re-Entry Aerodynamics*, AIAA, Inc., Washington DC, 1988.

INITIAL DISTRIBUTION LIST

		No. Copies
1.	Defense Technical Information Center Cameron Station Alexandria VA 22301-6145	2
2.	Library, Code 052 Naval Postgraduate School Monterey CA 93943-5002	2
3.	Dr. Rudolph Panholzer Chairman, Space Systems Academic Group Code SP Naval Postgraduate School Monterey CA 93943-5002 (DSN) 878-2948	1
4.	Dr. I. Michael Ross Code AA/RO Naval Postgraduate School Monterey CA 93943-5002 (DSN) 878-2948	8
5.	Dr. Sandra L. Scrivener Code AA/SS Naval Postgraduate School Monterey CA 93943-5002 (DSN) 878-2936	1
6.	Director, Navy Space Systems Division (N63) Space and Electronic Warfare Directorate Chief of Naval Operations Washington DC 20350-2000	1
7.	Dr. C.C. Chao Manager, Orbit Dynamics Section The Aerospace Corporation Post Office Box 92957 Los Angeles CA 90009-2957	1
8.	LT Daniel J. Cuff Tactical Air Control Squadron 22 FPO New York 09501-6542 (DSN) 680-8237	4